Evaluation of Ultra-Wideband Sensing Technology for Position Location in Indoor Construction Environments

by

Afrooz Aryan

A thesis

presented to the University of Waterloo

in fulfillment of the

thesis requirement for the degree of

Master of Applied Science

in

Civil Engineering

Waterloo, Ontario, Canada, 2011

AUTHOR'S DECLARATION

I hereby declare that I am the sole author of this thesis. This is a true copy of the thesis, including any required final revisions, as accepted by my examiners.

I understand that my thesis may be made electronically available to the public.

Abstract

Effective construction management involves real-time decisions regarding the progress of specific activities, the location of materials and equipment, and the construction site safety. The decision making process can be improved using real-time positioning technologies such as Radio Frequency Identification Device (RFID) systems, Global Positioning System (GPS), and Ultra Wide Band (UWB) sensors. While the GPS is not applicable to indoor positioning and RFID tags cannot provide a fully automated system for position location, the characteristics of UWB systems make this technology a strong candidate for a fully automated positioning system in an indoor construction environment. This thesis presents a comprehensive study of the performance of UWB systems in a controlled laboratory environment and in an institutional construction site in Waterloo, Canada as well as for a particular safety application. A primary objective of the research was to establish the accuracy of real-time position location under various conditions, including the effect of different construction materials (e.g., wood and metal), and to analyze changes in the accuracy of position location as construction progresses and the indoor environment physically evolves. Different challenges faced in implementing such a system in an active construction environment are addressed. Based on a statistical analysis of laboratory data, and considering the construction site experience, the reliability of the UWB positioning system for the aforementioned environments is discussed. Furthermore, an automated safety system is proposed using the real-time UWB positioning

technology. Based on the error modeling of the UWB position location, an optimum alarming algorithm is designed for the proposed safety system and the reliability of such system is evaluated through a statistical analysis.

Acknowledgements

I would like to take this opportunity to thank those who have helped me to complete this thesis. I would like to foremost thank my supervisor, Professor Ralph Haas, and my co-supervisor Professor Jeffrey West.

I was honored to work with Professor Ralph Haas, a worldwide known engineer in the field of transportation engineering, as my supervisor. I would like to thank him for giving me this opportunity to learn from him throughout the course of my study.

This thesis would not have been possible without Professor West's consistent guidance and support. I have had a great opportunity to work with him and have learned a lot from him.

I would like to thank the readers of my thesis, Professors Scott Walbridge, Jatin Nathwani, and Carl Haas for taking the time to carefully review my thesis, providing me with insightful questions and suggestions. I am also thankful to my colleague, Arash Shahi, for helping with the data collection for chapters 3 and 4.

I would like to acknowledge the National Science and Engineering Research Council of Canada (NSERC) financial support of this research study.

I would like to heartily thank my husband, Majid, whose unconditional love, patience, and support always helped me throughout my Master's study. My warmest gratitude goes to my parents who always encouraged me throughout my life.

Finally, I would like to thank my brother, Ashkan, my sister Azarm, and my wonderful friends with whom I spent many happy moments of my life.

This thesis is dedicated to my love, Majid,

and

to my dear parents.

Table of Contents

List of Figures

List of Tables

Chapter 1

Introduction

1.1 General

Construction management plays a critical role in successful civil engineering projects. Real-time data on construction activities is required for an effective management system. Information about the location of construction resources, such as workforce, equipment, and materials is highly beneficial to a manager in order to conduct different construction phases on time, safer, and within the allocated budget. A real-time positioning system can be a useful tool as part of construction management (Teizer et al., 2008).

Different position location systems are applicable in a construction site. Some available technologies are: Global Positioning Systems (GPS), Radio Frequency Identification Device (RFID), vision cameras, Laser Detection and Range tracking (LADAR), and Ultra Wide-Band (UWB).

UWB is a sensing technology which has been recently used in the construction industry. The system consists of UWB tags and receivers which communicate through UWB radio frequency signals. The 3-Dimensional (3-D) location of each tag can be recorded on a computer and the location and movement of each tag can be visually shown on a screen where the area under coverage of the sensors has been

already defined for the system. Different objects and persons on a construction site can be tagged and their real-time location and movement can be detected via a UWB location position system. This location information could help the project manager be aware of the location of any tagged object or person on site in order to use that information for either safety or management applications. It is also possible to track the progress of certain activities on site (e.g., piping installation) using this sensing technology.

1.2 **Research Objectives**

Use of UWB systems in construction management has been proposed in some recent work; however there have been only limited investigations in field applications. The performance of such a system in real construction sites has not been rigorously investigated. To evaluate the application of a UWB system for construction management, it is important to assess its performance in a real construction situation, and to determine the accuracy of the system when used in an environment with different construction material obstacles such as wood, metal, drywall, etc. Knowing the alternative challenges that might be expected for installing a UWB sensing system in a construction site will provide experience to compensate for the potential delays and problems associated with its use. The motivation of this research is to address these concerns.

1.3 Thesis Organization

In Chapter 2, previous studies and possible applications of the technology in construction management are presented. Different position location systems and their principles are also discussed. Furthermore, the different components of a UWB position location system are described.

In Chapter 3, a preliminary study on the performance of a UWB system in a controlled lab environment is reported and the results are presented. The effect of different factors (i.e., tag, cover, and location) on the accuracy of the UWB location reading has been also investigated.

In Chapter 4, an experimental set up in a real construction site is presented and recommendations regarding the installation of such a system are made. Some of the challenges the research group faced during the installation phase are also reported.

In Chapter 5, the application of a UWB system for safety purposes is investigated. In this chapter, a warning system to prevent potential accidents with a predefined reliability (e.g., 99.9%) has been modeled. In the first phase, error modeling for a UWB system installed in the structures laboratory at the University of Waterloo has been performed. Then in the second phase, an analysis to determine an algorithm for the alarm process has been conducted. To do so, the fundamental techniques of detection theory have been applied.

Chapter 6 presents calculations and recommended future work based on the findings of the current study.

Chapter 2

Background

The origin of UWB technology dates back to the 1960s, when its application was restricted to U.S. government and military programs. The Federal Communications Commission (FCC) approved the unrestricted use of low-powered UWB systems and tags (5 mW) in 2002; therefore non government-related research has increased in the last decade (Bennet &Ross, 1978; Breed, 2005; Ghavami et al., 2007; Tiezer 2008). According to the FCC, any signal with a relative bandwidth larger than 20% or absolute bandwidths greater than 500 MHz is considered as a UWB signal (Breed, 2005). With the extreme wide bandwidth, UWB positioning system is capable of covering a large area and also coexists with other wave frequencies at low or no interferences (Teizer et al., 2007; Teizer et al., 2008).

Use of UWB technology in real-time tracking of construction materials and resources is becoming more valuable because of the rising competition between construction companies, more accurate work performance demand, budget restrictions, and tighter schedules (Golparvar Fard, 2007; Teizer et al., 2008). Real-time tracking and location positioning are new methods which not only provide benefit for all project participants but also for all organizational levels. Workforce, project manager, field manager and executive managers all benefit from decisions

made based on real- time data. A practical data information system is supposed to be capable of providing information for different time intervals. The data is better to be in 3-D space and to be collected safely with a minimum cost. These rationales make the UWB positioning system a strong candidate for a real-time data collection system (Teizer et al., 2008).

2.1 Ultra Wide-Band Definition

According to the FCC, any signal with a relative bandwidth larger than 20% or absolute bandwidths greater than 500 MHz is considered as a UWB signal (Breed, 2005; Siwiak & McKeown, 2004).

2.2 UWB Historical Development

Most people would consider UWB as a new technology, since it provides the means to do what is possible only recently. Some of these new applications are: use of high data rates, and smaller, lower powered devices. However from an engineering perspective, UWB is not a new technology; because the applied physical properties are the ones that have been discovered before (Ghavami et al., 2007).

UWB radar system was one of the earliest applications of UWB in the military. Automobile collision avoidance, positioning system, liquid-level sensing, and altimetry are other applications, which were developed later. Most of the applications were restricted to U.S. government and military programs. The US Department of Defense was the first to use the UWB term as it was referred to as baseband, career-free and impulse technology in the early days. The late 1990s was when

commercialized UWB systems were introduced (Gu & Taylor, 2003; Ghavami et al., 2007; Siwiak & McKeown, 2004).

2.3 UWB Regulations

Some of the organizations and government entities that set rules and recommendations for use of UWB are (Ghavami et al., 2007):

- International Telecommunication Union (ITU)
- Asia Pacific Technology (APT)
- Federal Communication Commission (FCC) in the United States (US)
- Office of Communication (OFCOM) in the United Kingdom (UK)

The first country that legalized the commercial use of UWB was the USA. The FCC lifted certain limits on UWB in March 2005.

2.4 Ultra Wide- Band Advantages

UWB systems were mainly developed as radar systems for military applications. The main advantages for UWB systems are considered as low power, low cost, precise positioning with high data rate and very low interference with other available wireless systems. Advantages of the UWB systems are presented in the following section (Ghavami et al., 2007).

2.4.1 High Data Rates

Since UWB occupies an extremely large bandwidth, high data rates are available using these systems.

2.4.2 **Low Equipment Cost**

Eliminating many of the expensive components of conventional sinusoidal transmitters and receivers makes it possible to manufacture an inexpensive system.

2.4.3 **Multipath Immunity**

The extremely wide bandwidth that UWB system operates on makes the system robust to multipath effects caused by presence of obstacles. Because of the short pulses of the UWB, unwanted multipath reflections can be detected and filtered from the real UWB pulses.

2.4.3.1 **Multipath Effect**

Multipath is a phenomenon at the receiver which results in radio signals reaching the receivers by two or more paths. This effect is depicted in Figure 1 (Ghavami et al., 2007). In fact, objects between the signal transmitter and the receiver cause multipath propagation by reflecting, absorbing, diffracting and scattering of the signal energy. The pulses travel in different paths, and are received at the receiver with the delay proportional to the path length they have travelled (Ghavami et al., 2007).

2.4.4 **High Penetration Capability**

One of the most important advantages of UWB systems is that UWB signals can easily propagate through walls, doors, partitions, bricks, cement, and other obstacles (Ghavami et al., 2007).

2.4.5 **Low Power Consumption**

If the UWB system is properly designed, its power consumption could be quite low. The engineering design includes more efficient circuit designs and more signal processing done on smaller chips at lower operating voltage.

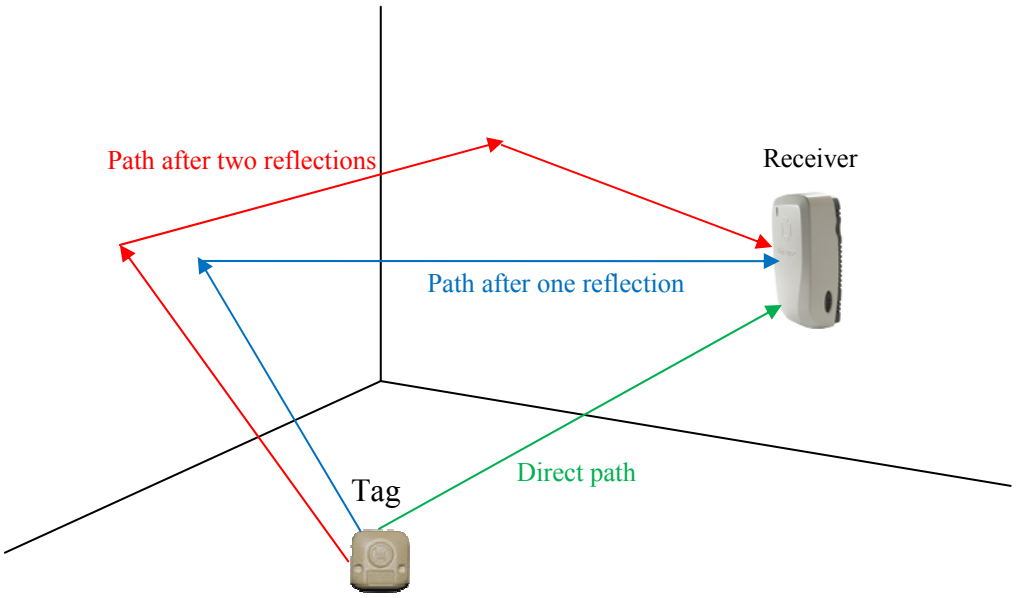

Figure 1: Multipath phenomenon.

2.5 Ultra Wide- Band Challenges

Like any new technology, there are some challenges associated with using UWB systems. Because of the very large bandwidth occupancy of UWB systems, different users whose spectrum will be affected are involved in use of this technology and it is necessary to have a regulation in order to avoid interference between different users. Therefore, the most obvious problem associated with this technology is regulatory (Ghavami et al., 2007).

Another problem is lack of standards on which the industry agrees to use to make the UWB devices interoperable. This standard gap limits the potential growth of the UWB market (Ghavami et al., 2007).

Although UWB promises a low-cost technology, low-power operation, resolving the interference problem may increase the cost of the technology (Ghavami et al., 2007).

2.6 Literature Review

Successful construction projects are the ones that often benefit from a higher level of awareness of the jobsite conditions. Recently, Ultra wide band (UWB) has been considered as an emerging technology for asset tracking in infrastructure management (Teizer et al., 2008). Having the 3-D location of the items and personnel moving in the site helps the project manager make fast and confident decision based on real-time data. Since the application of UWB positioning systems in construction management and safety systems is relatively new, there is not much works have been done in this area and the literature review is limited to some basic concepts and new articles.

Different positioning systems are applicable in a construction site. Some of available technologies are Global Positioning System (GPS), Radio Frequency Identification Device (RFID), vision cameras, Laser Detection and Range tracking (LADAR), and Ultra Wide-Band (UWB) sensing technology. Each aforementioned technology is briefly explained below (Teizer et al., 2008; Teizer et al., 2005; Razavi et al., 2010).

2.6.1 **Global Positioning Systems (GPS)**

GPS is a global navigation satellite system that requires an unobstructed line of sight to four or more GPS satellites to provide location information. Its widespread availability is an advantage for this technology. In the case that very accurate

positioning data is needed, higher installation and maintenance costs are involved. GPS application is limited to outdoors, because in an indoor environment, excess loss of signals and multipath effect decrease the accuracy of the system. Therefore, GPS could be a cost effective option for tracking the position of larger resources such as heavy equipment fleets (Bowes & Keefer, 2007; Teizer et al., 2008).

2.6.2 **Radio Frequency Identification Device (RFID)**

RFID has been considered as a technology for tracking construction materials since the mid-1990's. An RFID tag transfers radio frequency waves that enable the reader device to locate the tag position in 2 or 3 dimensions. Line of sight is not required for the system; therefore it can easily be adopted in construction projects where the presence of obstacles (e.g., walls, ceilings, etc.) prevents the tag to have a line of sight between the tag and the reader. This characteristic helps the durability of the tags when they can be encapsulated in waterproof cases or material packaging. Using this system, each tagged item has a distinct ID which enables the system to track items independently. There are two types of tags available: passive and active. Passive tags have no battery and their read range is short; on the other hand active tags are battery powered and benefit from high read range. The update rate for this technology is hourly or daily based and it is sufficient for applications such as inventory management. Recently the application of GPS- and RFID- based sensing systems has been investigated in construction material tracking and supply chain management. The size of such sensor systems is large and the weight is heavy. Furthermore, in order to have higher positioning accuracy the cost goes up. These systems are good to use on larger vehicles or materials but not on workforce (Razavi

et al., 2010; Song et al., 2006; Golparvar Fard & Peña-Mora., 2007; Teizer et al., 2008).

2.6.3 **Vision Camera**

Vision camera is a cost-effective technology which covers a large field of view of job sites remotely; however it requires line of sight. A source of illumination is also required when working at night. Since the video or images from the camera need to be processed, it is not well suited to automated tracking of materials in complex environments of construction job sites (Golparvar Fard & Peña-Mora., 2007; Brilakis, 2008; Teizer et al., 2008).

2.6.4 **Laser Detection and Range Tracking (LADAR)**

LADAR is applicable in a construction site in order to get a 3-Dimensional (3D) data from the entire site. Again the requirement for line of site is unfavorable for using this technology in construction environment. As well, 3D models taken from LADAR need to be processed to assist project manager efficiently (Teizer et al., 2008; Teizer et al., 2005).

2.6.5 **Ultra Wide-Band Sensing System**

Available technologies are useful to locate or track the workforce, equipment, and materials individually; but they are not appropriate to locate or track either all three at the same time (Teizer et al., 2008). UWB could be considered as an emerging technology in construction management which can address this issue and it is applicable in real-time location sensing and position tracking applications.

Proactive work zone safety has also been suggested as one of the UWB system applications in construction management (Teizer et al., 2008). Since safety is one of

the key objectives in any construction project, it is requires a real-time data collection system for this purpose. UWB system is applicable because of its longer read range that provides a larger coverage area, its coexistence with other radio technologies at low or no interference, and its capabilities that make it functional in object cluttered indoor construction sites (Teizer et al., 2007; Teizer et al., 2008).

There are a number of applications for UWB systems in work zone safety. Field personnel can make safer decisions using such a system. A worker who works close by or inside the swing radius of heavy equipment, and the equipment operator who has limited field of view can benefit from real-time data collected by the UWB system. Therefore, automatic 3-D real-time data acquisition system could be beneficial for safety applications in a construction project in order to warn personnel who work nearby of the hazardous construction zones with making alarms when violating work boundaries. Such a system can prevent or reduce accidents, injuries, and fatalities from happening (Teizer et al., 2007; Teizer et al., 2008).

In one of the most recent studies about UWB location position systems (Yong, 2010), the accuracy of UWB location measurements in two different static and dynamic tests is calculated. For the static test, the results show that the accuracy of measurements in both wood-framed building and steel-framed building are better when the tags were positioned about a meter above the floor rather than on the floor. This is due to the better line of sight of the sensors. The authors claim that there is no significant difference in accuracy in wood-framed building compared to a steel-framed building. It is also claimed the accuracy is more sensitive to location and facing angle of sensor nodes. In a dynamic test, Kalman filtering was used to build an

error model. Using this filter the current location of the tag can be more accurately estimated based on the previous state of the tag (Yong, 2010).

UWB asset location systems have been previously used in hospitals, military facilities, warehouses, and factories; but its application in infrastructure construction is new. Potential applications and research topics of UWB in this area have been addressed in the literature as (Teizer et al., 2008; Teizer et al., 2005):

- Supply chain and asset management
- Work zone safety
- Robotics and automation
- Security applications
- Field data communication
- Search and rescue operations
- Data processing algorithms
- Simulations
- Impact analysis

2.7 **Position Location System Classification**

One type of position location system classification is based on the place where readings and calculations take place. According to this classification, there are three system categories (Ghavami et al., 2007).

2.7.1 Classification Based on Type

2.7.1.1 Network-Based Systems

In network-based systems, a signal reflected from the target which is going to be positioned is read by a set of receivers. Then the calculations to position the target take place in a control station located different from the measuring space.

2.7.1.2 Handset-Based Systems

In handset-based systems, location-known transmitters send signals to the positioning receiver and the receiver uses the measurements to determine its own position.

2.7.1.3 Hybrid Systems

Hybrid systems are a combination of the previous two systems. The object to be located usually takes the measurements and transmits the data. The object position is calculated in a stationary network. This method enables the system to achieve a more robust estimate of location in a single process.

2.7.2 Classification Based on Operating Frequency

2.7.2.1 Frequency-Based Systems

In addition to this classification, wireless positioning systems can be classified by their operating frequency as well. Higher frequency leads to a more accurate positioning system. Operating frequency determines the accuracy of the system and the operating range; therefore, it enables the user to decide if the system is proper for a particular application or not. The systems for tracking people and objects in an indoor environment (e.g., UWB location positioning systems) use high frequency and bandwidth radio signals. Based on this criterion positioning systems are categorized as (Ghavami et al., 2007):

- Low-frequency positioning systems (30 KHz–300 KHz)
- Medium-frequency positioning systems (300 KHz to 3 MHz)
- Super-high-frequency positioning systems (between 3 and 30 MHz)

2.8 Network-Based Positioning Techniques

There are four types of network-based techniques for location positioning, which are briefly introduced in the following section. The four techniques are: time of arrival (TOA), time difference of arrival (TDOA), angle of arrival (AOA) and received signal strength (RSS) (Ghavami et al., 2007; Munoz, 2009).

2.8.1 Time of Arrival (TOA)

In this technique, the receiving time of the signals transferred by the target object is measured at each receiver. The propagation time of the signal is known and has a direct relation with the distance the signal travels. Therefore the distance between the object and the receiver can be calculated resulting in a circle centered at the receiver with its radius representing the calculated distance. A minimum of three circles is required for a 2-Dimensional (2D) positioning system. If the coordinates associated with the three receivers are known, the position could be calculated. To simplify the formulation, we assume Receiver 1 is located on the origin of the coordinates and the y axis is defined by the line connecting Receiver 1 and Receiver 2. Therefore, the receiver coordinates are (Ghavami et al., 2007; Munoz, 2009):

Receiver 1: (0, 0)

Receiver 2: (0, y_2)

Receiver 3: (x_3, y_3)

The TOA positioning principle is illustrated in Figure 2.

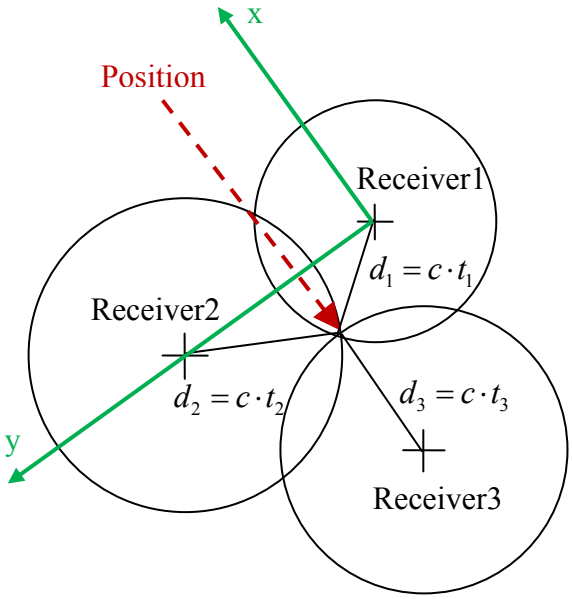

Figure 2: TOA positioning principle.

The signal speed of propagation is taken as c and the duration that the signal takes to travel between the object and the respective receivers is shown as t_1, t_2, and t_3. The distances between the tag and each receiver can be calculated as:

$$d_1 = c \cdot t_1 = \sqrt{x^2 + y^2} \tag{2.1}$$

$$d_2 = c \cdot t_2 = \sqrt{x^2 + (y - y_2)^2} \tag{2.2}$$

$$d_3 = c \cdot t_3 = \sqrt{(x - x_3)^2 + (y - y_3)^2} \tag{2.3}$$

Each of the above equations defines an unknown circle. From the above equations and doing some basic manipulation we have:

$$y = \frac{(y_2^{\,2} + d_1^{\,2} - d_2^{\,2})}{2y_2} \tag{2.4}$$

Substituting this value in Equation (2.1), two values for x are found, but only the one which satisfies the Equation (2.3) is acceptable. This way the desired position is found.

2.8.2 **Time Difference of Arrival (TDOA)**

In this technique, the difference between arrival times of the signals to two different receivers from the object to be positioned is measured. Each time difference represents a hyperboloid in which the constant distance is the distance between the two corresponding receivers. For a 2-D positioning system, at least two hyperboloids (i.e., two pairs of receivers) are required. The position of the object is defined as the intersection of these two hyperboloids. For example, assume the coordinates of the receivers to be (Ghavami et al., 2007; Munoz, 2009):

Receiver 1: (0, 0)

Receiver 2: (0, y_2)

Receiver 3: (x_3, y_3)

The time duration that the signal travels between the object and the respective receivers are t_1, t_2, and t_3; then calculation of the position would be as follows:

$$d_1 = c \cdot t_1 \tag{2.5}$$

$$d_2 = c \cdot t_2 \tag{2.6}$$

$$d_3 = c \cdot t_3 \tag{2.7}$$

Using the TDOA algorithm two hyperboloids are defined.

$$d_{1,2} = d_2 - d_1 = c \cdot (t_2 - t_1) = \sqrt{x^2 + (y - y_2)^2} - \sqrt{x^2 + y^2} \tag{2.8}$$

and

$$d_{1,3} = d_3 - d_1 = c \cdot (t_3 - t_1) = \sqrt{(x - x_3)^2 + (y - y_3)^2} - \sqrt{x^2 + y^2} \tag{2.9}$$

Taking the square in Equations (2.8) and (2.9) we have

$$2d_{1,2}\sqrt{x^2 + y^2} = {y_2}^2 - d_{1,2}^2 - (2y_2)y \tag{2.10}$$

$$2d_{1,3}\sqrt{x^2 + y^2} = {x_3}^2 + y_3^2 - d_{1,3}^2 - (2x_3)x - (2y_3)y \tag{2.11}$$

Knowing that $x^2 + y^2 \neq 0$ it can be derived from Equations (2.10) and (2.11) that

$$x = by + a \tag{2.12}$$

where

$$b = \frac{2y_2 d_{1,3} - 2y_3 d_{1,2}}{2x_3 d_{1,2}} \tag{2.13}$$

and

$$a = \frac{x_3^2 d_{1,2} + y_3^2 d_{1,2} - y_2^2 d_{1,3} - d_{1,2} d_{1,3}^2}{2x_3 d_{1,2}} \tag{2.14}$$

Substituting Equation (2.12) into Equation (2.10) leads to

$$2d_{1,2}\sqrt{(b^2 + 1)y^2 + (2ba)y + a^2} = y_2^2 - d_{1,2}^2 - (2y_2)y \tag{2.15}$$

which results in

$$[4d_{1,2}^2(b^2 + 1) - 4y_2^2]y^2 + [8bad_{1,2}^2 + 4(y_2^2 - d_{1,2}^2)y_2]y + [4a^2 d_{1,2}^2 - (y_2^2 - d_{1,2}^2)^2] = 0 \tag{2.16}$$

Equation (2.16) is a quadratic equation. It has two roots that are the y-coordinates of the intersection points of the hyperboloids. Using Equation (2.12) provides the corresponding x-coordinates. We can define another hyperboloid by

$$d_{2,3} = d_3 - d_2 = c \cdot (t_3 - t_2) = \sqrt{(x - x_3)^2 + (y - y_3)^2} - \sqrt{x^2 + (y - y_2)^2} \tag{2.17}$$

Substitution of $d_{1,3}$ and $d_{2,3}$ in equations (2.10)-(2.16) yields two points. One of the two points matches the previous points. This point is the desired position we are looking for (Ghavami et al., 2007). The TDOA positioning principle is shown in Figure 3.

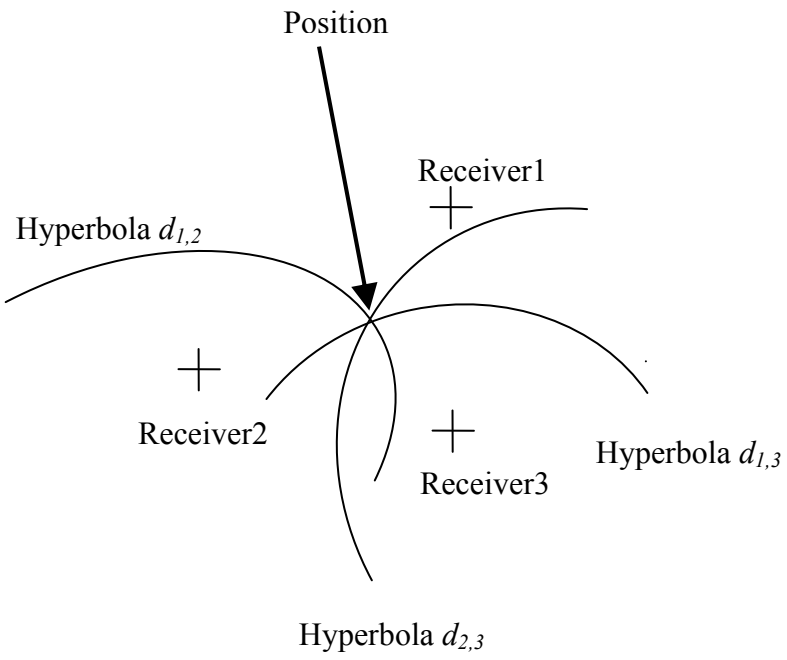

Figure 3: TDOA positioning principle.

2.8.3 **Angle of Arrival (AOA)/ Direction of Arrival (DOA)**

In this technique, several stationary receivers measure the angle of arrival of the signal sent by the target object. Each measurement provides a radial line from the receiver to the object. In a 2-D positioning system, the intersection of two dimensional lines of bearing defines the position of the object. In practice, the use of more than two receivers increases the system accuracy and reduces multipath propagation effects. The AOA positioning principle is shown in Figure 4.

Assume that the coordinates of the receivers are (Ghavami et al., 2007):

Receiver 1: (0, 0)

Receiver 2: (0, y_2)

Considering α and β, respectively, as the angles of arrival of the transmitted signal received at Receiver 1 and Receiver 2 respectively, the two straight lines in Figure 4 are defined by:

$$y = \tan(\alpha) \cdot x \tag{2.18}$$

$$y = \tan(\beta) \cdot x + y_2 \tag{2.19}$$

Substituting the calculated x_0 in Equation (2.19), a unique y_0 is defined, and thus the desired point is defined by (x_0, y_0) coordinates.

2.8.4 **Received Signal Strength (RSS)**

In this technique, each receiver measures the signal strength of the target object. Each measurement defines a circle centered at the receiver and the radius of the circle is the distance between the object and the receiver. The intersection of these circles defines the object position. The accuracy of the positioning system is increased as the

number of measurements increases. An example of RSS positioning is shown in Figure 5 (Ghavami et al., 2007).

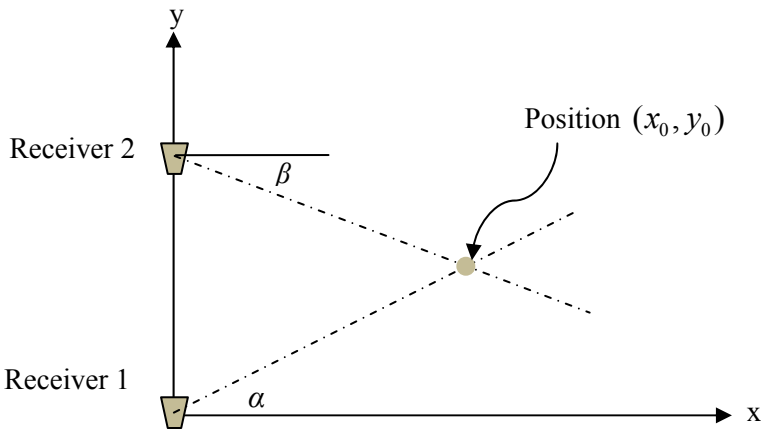

Figure 4: AOA positioning principle.

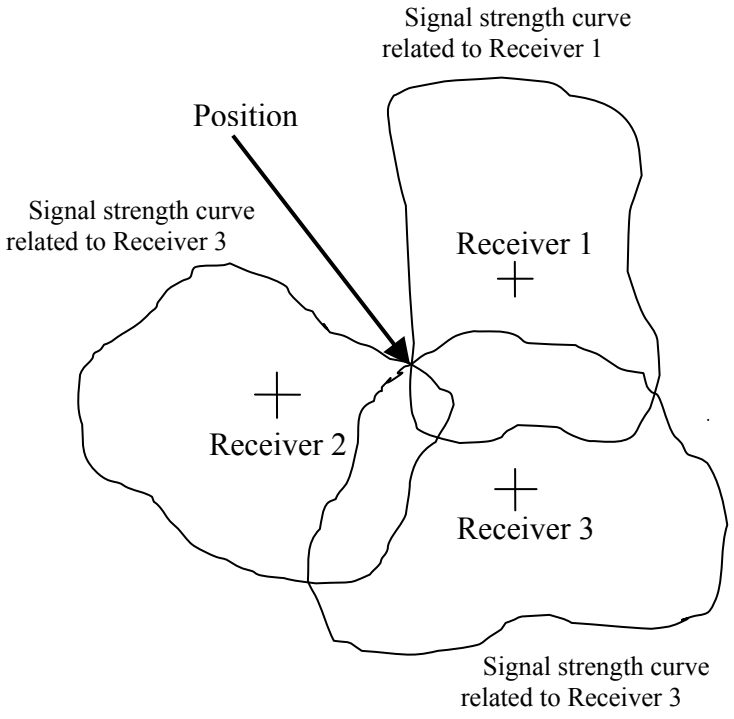

Figure 5: RSS positioning principle.

2.9 UWB System Components

In general, a UWB system consists of: receivers, tags, CAT-5e cables, power over Ethernet (POE) switch, and a graphical user interface installed on a computer. A tag transmits UWB pulses and the receivers are able to receive the pulses through their antennas. The receivers are connected to each other and to the POE switch through CAT-5e cables. One master sensor will be introduced to the system. Any other receiver in that cell is considered as A slave sensor. The master is the receiver, which enables the system to calculate the location for a tag.

A UWB receiver is a device utilized by an antenna that receives the UWB signals transmitted by a tag. The antenna is encapsulated in a plastic cover. A typical UWB receiver is depicted in Figure 6. The cross on the receiver case shows the location of the antenna under the cover.

Figure 6: UWB receiver; the cross shows the antenna location under the cover.

Each receiver has six ports (input/output) on its back. The timing cables are plugged into these ports. There is also a single port on the lower left side of the back, which is the power port. The CAT-5e cable from the POE switch is plugged into this port to provide the power for the sensor. A schematic diagram of a UWB system set up is shown in Figure 7. The view range of the receivers is 120° horizontally and 100° vertically. In order to calculate tag location, it is required that at least two of the receivers have a clear line of sight to the tag. Site survey measurements dictate the maximum distances a tag could have from the receivers in order to be located. Metal surfaces produce a lot of interruption to the system, which make it unable to work properly; therefore the receivers should be installed away from metal surfaces. It is recommended to install the sensors as high as possible but lower than potential obstacles.

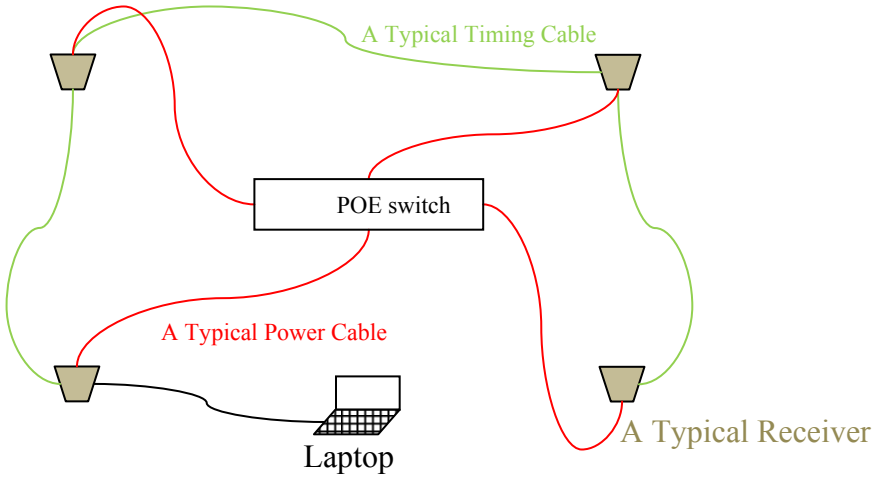

Figure 7: A schematic diagram of a UWB system setup.

The UWB system applied in this study consists of UWB tags and UWB receivers (sensors) from the Ubisense® Company. As mentioned before, there are four types of techniques applied for position location: time of arrival (TOA), time difference of arrival (TDOA), angle of arrival (AOA) and received signal strength (RSS) (Ghavami et al., 2007; Munoz, 2009). A UWB system can be used as a real- time positioning system, which detects the 3-D coordinates of a tag. The system used in this study uses both TDOA and AOA techniques which increases the accuracy of location estimation.

The UWB positioning system used is a network of tags and sensors communicating over 6-8 GHz signals. To locate a tag, the path from transmitter to receiver has to be measured. Direct path signals determine the true location; however the reflections of the signal produce error. With UWB signals the reflections can be distinguished from the direct path and consequently the system is more accurate. The coordinates of the receivers are defined by total station surveying measurements. One master sensor which computes the final location of the tag and reports its coordinates to the server is introduced to the system. Each tag transmits UWB pulses which enable the sensors to compute the time difference of arrival and angle of arrival. Any two pieces of information (e.g., two AOAs or one AOA and one TDOA) enables the system to compute a tag position. Therefore a tag can be detected by only two sensor sightings. In practice, more sensors measurements enable the system to locate the tags more accurately which leads to a more robust system.

Two types of tags were provided in the UWB system package used in the current study: compact and slim tags. A compact tag usually attaches above the object to be tracked. The tag signal update rate can be adjusted depending on its movement speed;

the faster the tag moves, the higher update rate is required. A slim tag usually attaches to the side of the object and has programmable button and LED for different applications. An event can be generated on the server by pressing the button

A slim tag, a compact tag and a receiver are depicted in Figure 8. The tags are identified by a number on their barcode, which is shown in Figure 9.

Each receiver is required to be connected to other receivers in the system and to a POE switch as well. The connection is through CAT-5e cables which transfer both data and power. Figure 9 shows how the timing and the power cables should be plugged into the receivers. POE port is located on the bottom left, and timing input port is the upper right port.

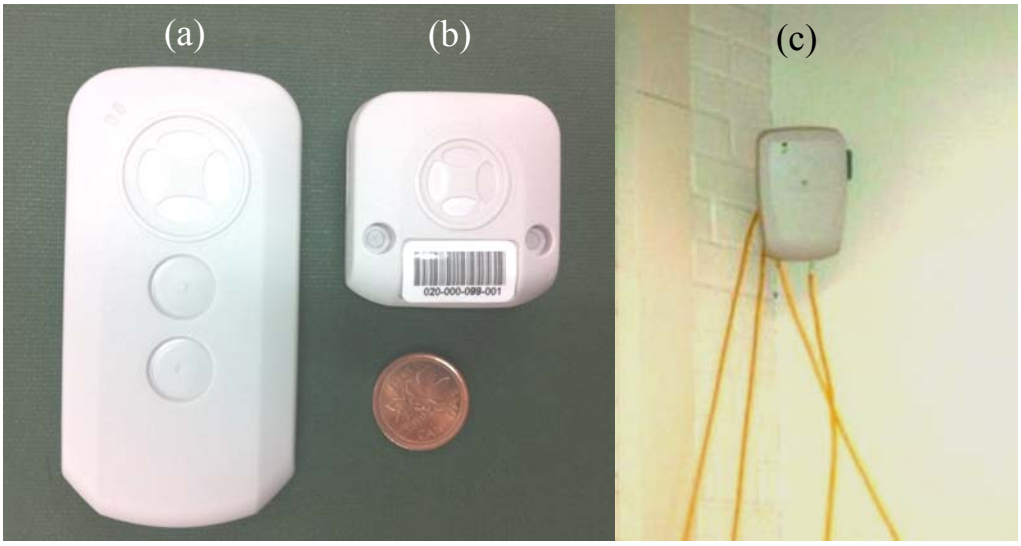

Figure 8: (a) Slim tag, (b) Compact tag, (c) Receiver.

Figure 9: Timing and POE ports, and barcode on the back of the receiver.

2.10 **UWB Receiver Connection Methods**

There are two major types of topologies for receiver connections. The first one is the star topology which consists of a central receiver to which all other receivers are connected. The central receiver is called the master and enables the system to calculate a tag position. Any other receivers on the network are called slaves. The second type of connection is daisy chain in which each receiver is connected in series to the next receiver (Razavi et al., 2010). Figures 10 and 11 show these two connection configurations.

In the first part of the current study (Chapter 3), seven receivers were connected in a daisy chain configuration. In the second part (Chapter 4), four receivers were connected in a daisy chain. Finally in the last part of the study, four receivers were connected in a star topology.

It is recommended that for a daisy chain configuration, the number of the receivers connected to each other on each side of the master sensor is better to be

limited to maximum of 10 (because of the timing data accuracy). For the laboratory set ups in this research (Chapter 3 and Chapter 5), based on the size of the coverage area, both daisy chain and star topologies are applicable; but in the field set up (Chapter 4), the daisy chain is preferable because it reduces the required length of the cables and results in a simpler configuration.

2.11 Calibration Process

Calibration is a process that enables the system to calculate the sensor locations with respect to each other using a predefined coordinate. In order to get accurate object position data, it is necessary to calibrate the system properly. There are four types of calibration techniques:

- Orientation calibration: this technique is used to calibrate only yaw and pitch of a given sensor.
- Equidistance calibration: using this method it is required to place a tag where it has equal distances from two sensors.
- Dual calibration: this technique calibrates yaw, pitch, and cable offset for the two sensors involved in the process.
- Cable calibration: this method only calibrates the timing offset of a given sensor.

For the UWB system used in this research, the dual calibration process is applied since it was recommended by the Ubisense® Company.

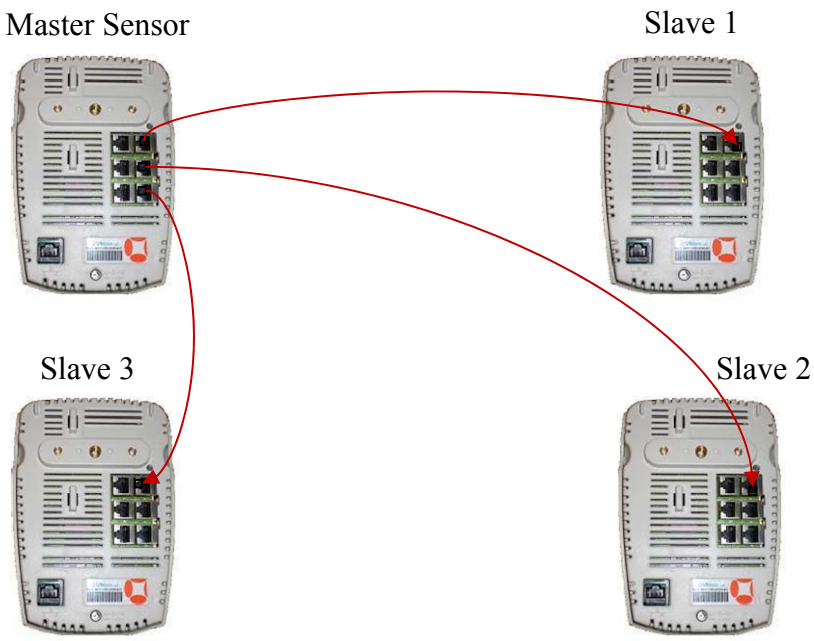

Figure 10: Star connection in which the master is the central receiver.

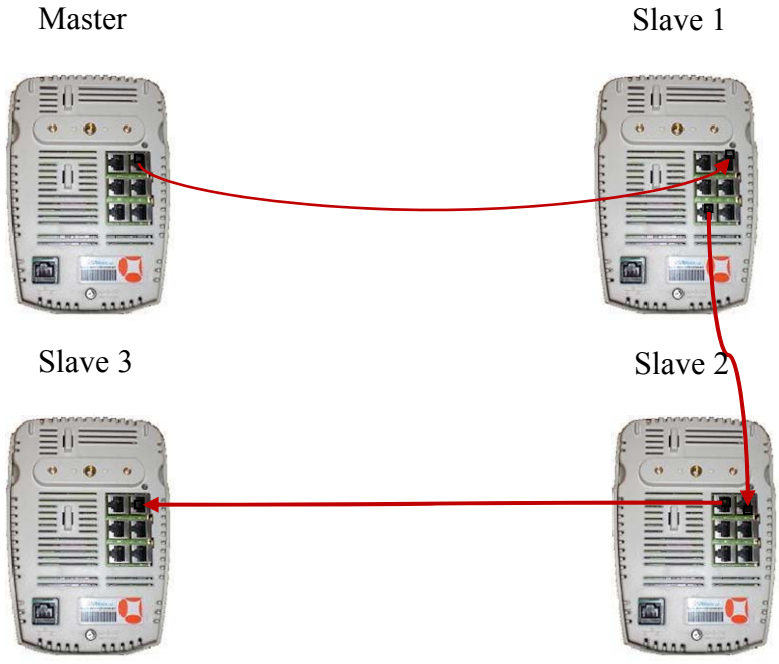

Figure 11: Daisy chain connection in which each receiver is connected in series to the next receiver.

2.11.1 **Dual Calibration**

The most commonly used calibration technique is dual calibration. For this technique, it is required that the tag has a clear line of sight to two sensors. One of the sensors is preferred to be the master, or a sensor that has already been calibrated with respect to the master is chosen. One tag (slim or compact) is placed on a known coordinate. The master's coordinate is also known by a total station measurement. Given the tag and the master coordinates, the slave sensor's coordinate can be calculated by the system.

Since the compact tag is omni-directional, the tag's orientation is not important. If the slim tag is used in the calibration process, then it is necessary to locate the tag in a position such that the face of the tag aligns with the master sensor and the slave sensor that is to be calibrated.

Chapter 3

UWB Position Location in the Vicinity of Different Materials

In this chapter, the results of a preliminary study on UWB system accuracy are presented, and the effect of different construction materials such as metal and wood on the system accuracy has been compared.

In the initial stage of this research, a preliminary study was conducted on the performance of UWB systems in real-time location sensing for a controlled environment. This stage provided a statistical evaluation of the UWB positioning system accuracy. Furthermore, the influences of three specific factors (i.e. tag, location, and cover) on the accuracy of UWB system is investigated.

3.1 Experimental Setup

The experimental program of this research was conducted in the sensing lab located at E3 building at the University of Waterloo. Eight UWB receivers were installed around the perimeter of the lab and connected in a daisy chain configuration using CAT-5e shielded wires. A laptop connected to a POE switch fed by the master sensor recorded the readings from all tags locations. UWB tags were placed in specified locations within the sensing lab, and their positions in the form of 3-D

coordinates (x,y,z) were recorded by the system at the exact time of the reading. To have a better estimate of the tag coordinates, we decided to record 15 measurements for each tag location and then average these measurements.

The layout of the sensors in the sensing lab environment is shown in Figure 12. This illustration is a screenshot from the licensed software used to monitor the tag [Location Engine Configuration software from the Ubisense® Company]. The screenshot depicts the outline of the lab and the receivers. The receivers are indicated by the red rectangles at the vertices of the shaded region. These receivers are directed inward and downward, thus forming a region where tags can be sensed. The red dot with green lines radiating from it represents a tag. The green lines represent the impulses radiating from the tag, and received by the receivers. The system uses these impulses to calculate the position of the tag in real- time.

3.1.1 **Data Collection**

To address the objectives of this experimental set up, the performance of the UWB system in the presence of different material obstacles was investigated. Only compact tags were used in this study. The obstacles were modeled as boxes with one open side. The boxes were made of various construction materials. The UWB tag was covered with the boxes and the tag positions were recorded by the system. The four levels of cover factor included in the experiment were: none, wood box, metal box, and RF shield box. Electromagnetic shielding used to block radio frequency (RF) radiation is known as RF shielding. The RF shield box keeps the RFID tags isolated and the one used in this study was made of steel. The RF-shield box is used in this

study to model a metal obstacle, which highly interferes the UWB system. Figure 13 depicts different covers used in this experiment.

The accuracy of the system has been introduced as a factor to assess the system performance. Therefore, all UWB readings for a particular point were compared to the exact location of that point as measured by a total station survey, and the difference between the two locations is considered as a representative of the "error" response variable. As the error magnitude increases, the accuracy of the measurements decreases. Considering x_t, y_t, and z_t as true coordinates measured by a total station surveying equipment and x, y, and z as the coordinates detected by the UWB system, the following formula was applied to calculate the response variable, "error":

$$E_{xyz} = \sqrt{(x - x_t)^2 + (y - y_t)^2 + (z - z_t)^2} \tag{3.1}$$

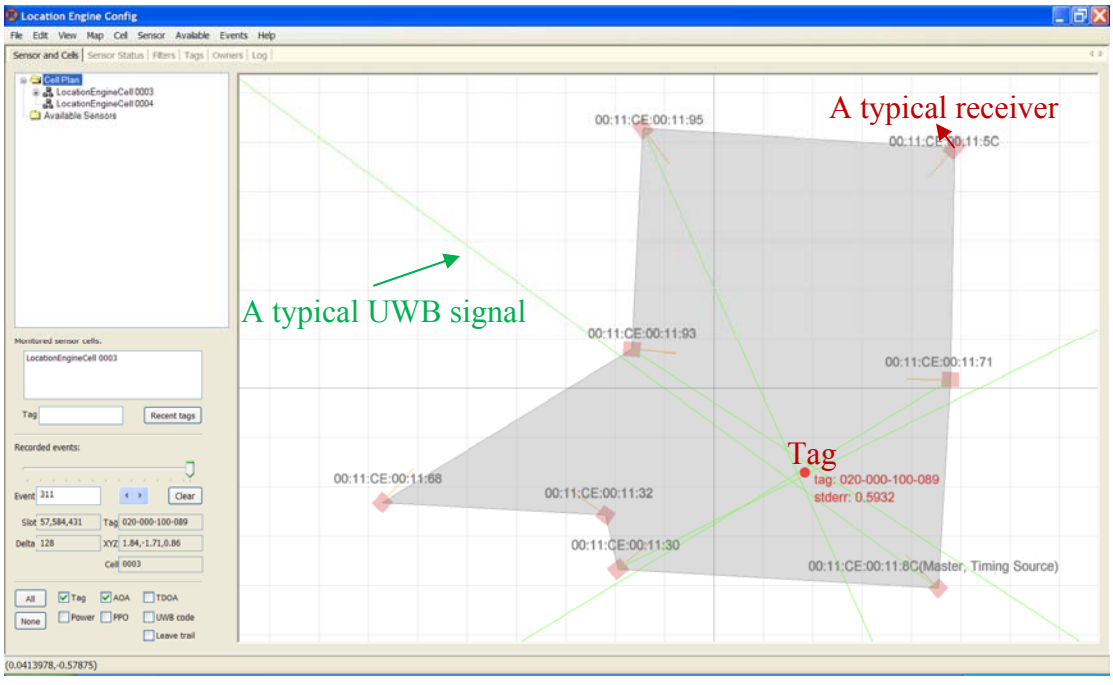

Figure 12: The UWB system layout for the experimental set up in the sensing lab.

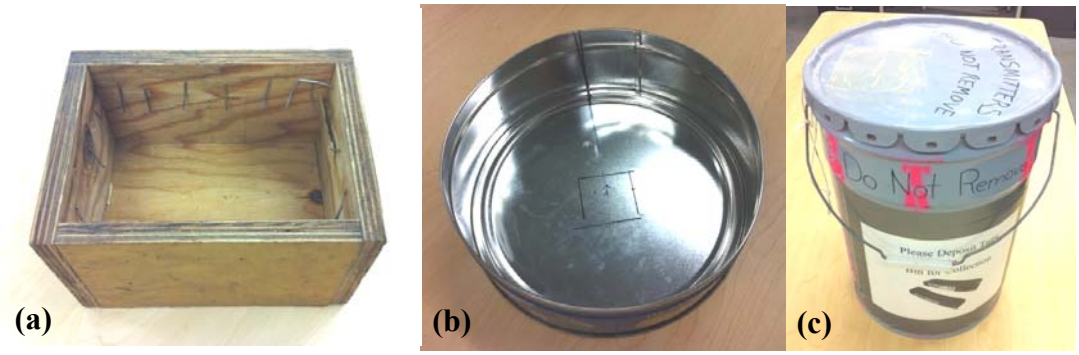

Figure13: Different covers used in the experiment: (a) wood box, (b) metal box, (c) RF-shield box

As mentioned before, 15 individual measurements are included in each sample. Therefore the response variable is the average of the 15 calculated errors. For each tag-cover configuration, four sets of measurement were taken, each consisting of 15 coordinate measurements. Each observation was taken under i^{th} tag, j^{th} cover, and at the k^{th} trial where i,j, and k are ranging from 1 to 4. Therefore the total number of observations is $4\times4\times4=164$. The results and analysis on average error are presented and discussed in this chapter.

The experiment was conducted during a two day period. Each tag has a distinct barcode, which enables the user to recognize that tag. Tag "i" is placed on top of a predefined point in the room and cover "j" is used as the tag's cover. Then 15 measurements of position readings of that special tag were recorded. The average of those 15 observations is then compared against the "true location" of the tag (obtained by total station reading), and the difference in terms of the 3D distance (E_{xyz}) is calculated using Equation (3.1). Tables 1 to 4 show the calculated E_{xyz} at four different locations and under 16 (4×4) different tag-cover configurations.

Figure 14 depicts the true locations of the four predefined points in the lab. These coordinates were determined using the total station surveying equipment.

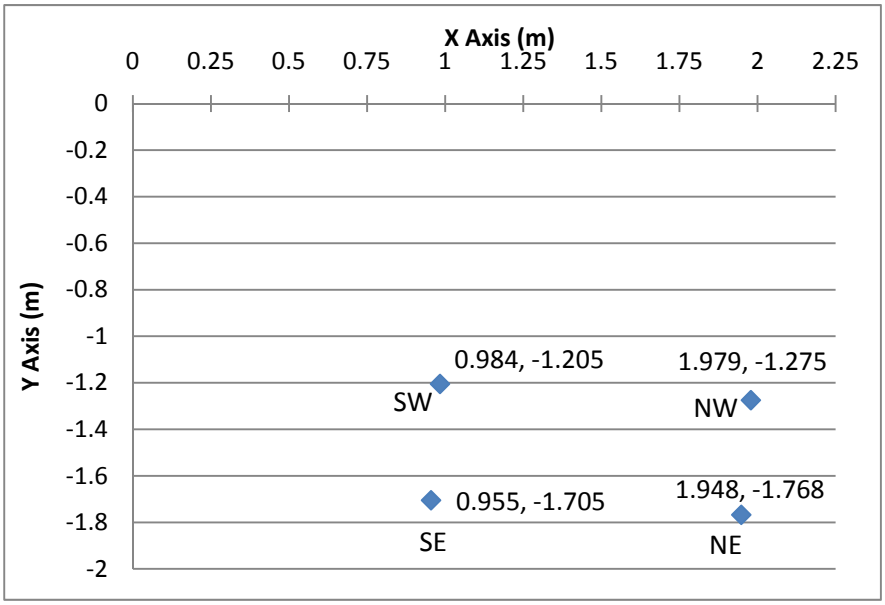

Figure 14: True location of the four predefined points in the sensing lab.

3.2 Results and Recommendations

This experiment includes a study on effects of three factors; the considering factors are: cover, tag, and location. A factorial design is the most efficient method for this experiment. In a factorial design experiment, each complete trial of the experiment investigates all possible combinations of the factors for different levels of each factor (Montgomery, 2001). The effect of factor is defined as change in the response variable (i.e., average error) when the level of the factor changes. This is called the main effect (Montgomery, 2001).

Table 1: Average error measurements (Ave.E_{xyz}) (in meters) without cover.

Tag#		No Cover			
	Obs. #	Point 1	Point 2	Point 3	Point 4
Tag #1	1	0.146	0.166	0.118	0.134
	2	0.167	0.156	0.108	0.138
	3	0.154	0.137	0.104	0.148
	4	0.176	0.142	0.137	0.127
Tag #2	1	0.126	0.124	0.068	0.119
	2	0.121	0.123	0.087	0.096
	3	0.127	0.115	0.087	0.108
	4	0.129	0.125	0.065	0.134
Tag #3	1	0.171	0.169	0.138	0.156
	2	0.189	0.166	0.124	0.150
	3	0.177	0.148	0.134	0.132
	4	0.175	0.163	0.152	0.136
Tag #4	1	0.170	0.148	0.130	0.114
	2	0.135	0.155	0.114	0.144
	3	0.160	0.151	0.114	0.145
	4	0.151	0.164	0.113	0.141

Table 2: Average error measurements (Ave.E_{xyz}) (in meters) for wood box.

Tag#		Woodbox			
	Obs. #	Point 1	Point 2	Point 3	Point 4
Tag #1	1	0.209	0.108	0.083	0.141
	2	0.208	0.111	0.091	0.093
	3	0.177	0.089	0.097	0.073
	4	0.165	0.094	0.105	0.095
Tag #2	1	0.216	0.087	0.104	0.083
	2	0.169	0.097	0.101	0.093
	3	0.174	0.091	0.100	0.088
	4	0.195	0.074	0.067	0.081
Tag #3	1	0.211	0.117	0.130	0.149
	2	0.202	0.140	0.107	0.122
	3	0.220	0.132	0.127	0.112
	4	0.202	0.136	0.135	0.114
Tag #4	1	0.195	0.123	0.108	0.102
	2	0.179	0.125	0.121	0.092
	3	0.204	0.125	0.089	0.121
	4	0.185	0.108	0.109	0.115

Table 3: Average error measurements (Ave.E_{xyz}) (in meters) for metal box.

Tag#		Metal Box			
	Obs. #	Point 1	Point 2	Point 3	Point 4
Tag #1	1	0.991	1.563	0.674	1.017
	2	0.240	0.762	0.860	0.985
	3	0.226	0.850	0.615	1.246
	4	0.225	0.404	0.517	1.219
Tag #2	1	0.263	0.253	0.909	0.309
	2	0.209	0.190	0.394	0.402
	3	0.287	0.160	0.464	0.223
	4	0.245	0.222	0.561	0.257
Tag #3	1	0.385	0.460	0.408	0.749
	2	0.223	0.286	0.491	0.609
	3	0.747	0.305	0.557	0.398
	4	0.591	0.230	0.407	0.725
Tag #4	1	0.156	0.248	0.896	0.445
	2	0.174	0.429	0.776	0.386
	3	0.170	0.448	0.768	1.380
	4	0.175	0.799	0.901	0.460

Table 4: Average error measurements (Ave.E_{xyz}) (in meters) for RF-shield box.

Tag#		RFID Box			
	Obs. #	Point 1	Point 2	Point 3	Point 4
Tag #1	1	0.876	0.391	0.462	0.635
	2	0.474	0.443	0.529	0.483
	3	0.874	0.462	0.391	0.482
	4	0.638	0.410	0.425	0.545
Tag #2	1	0.287	0.464	0.719	0.858
	2	0.494	0.573	0.537	0.623
	3	0.470	0.649	0.487	0.597
	4	0.444	0.540	0.460	0.833
Tag #3	1	1.133	0.406	0.442	0.771
	2	0.852	0.565	0.512	0.585
	3	0.707	0.390	0.440	0.720
	4	0.626	0.424	0.437	1.118
Tag #4	1	0.544	0.532	0.594	0.466
	2	0.655	0.510	0.527	0.473
	3	0.703	0.578	0.596	0.676
	4	0.649	0.591	0.440	0.463

At each location, 15 UWB readings are recorded, and then the average of the 15 measurements is compared to the true coordinates measured by a total station surveying equipment.

Average error and standard deviation for different data sets are presented in tables 5 to 8.

Table 5: Average error (Ave.E_{xyz}) & standard deviation for wood box data

	Wood Box	Location 1	Location 2	Location 3	Location 4
Tag# 1	Ave. E_{xyz}	0.185	0.096	0.084	0.097
	Stdev. E_{xyz}	0.025	0.009	0.009	0.029
Tag# 2	Ave. E_{xyz}	0.185	0.096	0.084	0.097
	Stdev. E_{xyz}	0.025	0.009	0.009	0.029
Tag# 3	Ave. E_{xyz}	0.205	0.128	0.115	0.119
	Stdev. E_{xyz}	0.011	0.012	0.012	0.015
Tag# 4	Ave. E_{xyz}	0.186	0.114	0.095	0.104
	Stdev. E_{xyz}	0.011	0.007	0.016	0.013

Table 6: Average error (Ave.E_{xyz}) & standard deviation for metal box data

	Metal Box	Location 1	Location 2	Location 3	Location 4
Tag# 1	Ave. E_{xyz}	0.388	0.733	0.607	0.902
	Stdev. E_{xyz}	0.372	0.404	0.137	0.232
Tag# 2	Ave. E_{xyz}	0.180	0.162	0.475	0.225
	Stdev. E_{xyz}	0.036	0.036	0.206	0.068
Tag# 3	Ave. E_{xyz}	0.463	0.252	0.404	0.562
	Stdev. E_{xyz}	0.226	0.041	0.062	0.142
Tag# 4	Ave. E_{xyz}	0.133	0.420	0.755	0.526
	Stdev. E_{xyz}	0.021	0.218	0.094	0.570

Table 7: Average error (Ave.E_{xyz}) & standard deviation for no-cover data

	No Cover	Location 1	Location 2	Location 3	Location 4
Tag# 1	Ave. E_{xyz}	0.155	0.143	0.110	0.133
	Stdev. E_{xyz}	0.013	0.015	0.011	0.009
Tag# 2	Ave. E_{xyz}	0.125	0.117	0.071	0.108
	Stdev. E_{xyz}	0.003	0.006	0.016	0.024
Tag# 3	Ave. E_{xyz}	0.174	0.158	0.125	0.138
	Stdev. E_{xyz}	0.008	0.009	0.010	0.013
Tag# 4	Ave. E_{xyz}	0.147	0.150	0.114	0.132
	Stdev. E_{xyz}	0.013	0.005	0.010	0.017

Table 8: Average error (Ave.E_{xyz}) & standard deviation for RF-shield box data

	RF-shield	Location 1	Location 2	Location 3	Location 4
Tag# 1	Ave. E_{xyz}	0.674	0.374	0.274	0.478
	Stdev. E_{xyz}	0.213	0.009	0.073	0.082
Tag# 2	Ave. E_{xyz}	0.377	0.471	0.444	0.587
	Stdev. E_{xyz}	0.105	0.045	0.131	0.175
Tag# 3	Ave. E_{xyz}	0.527	0.378	0.290	0.470
	Stdev. E_{xyz}	0.175	0.088	0.084	0.183
Tag# 4	Ave. E_{xyz}	0.497	0.516	0.418	0.431
	Stdev. E_{xyz}	0.035	0.042	0.043	0.045

The average error associated with each cover at each location is presented in Table 9.

Table 9: Average error (Ave.E_{xyz}) in meters for different covers and locations

Cover	Location 1	Location 2	Location 3	Location 4	**Ave. E_{xyz} (cover)**
Wood	0.190	0.103	0.095	0.099	**0.122**
Metal	0.291	0.392	0.560	0.554	**0.449**
Nothing	0.151	0.142	0.105	0.128	**0.131**
RFID-shield	0.519	0.435	0.357	0.492	**0.451**
Ave. E_{xyz} (Location)	**0.211**	**0.212**	**0.253**	**0.260**	

The average error associated with each cover is depicted in Figure 15. The figure shows that, average errors corresponding to the no cover and wood box cover are

relatively low, regardless of the used tag. The error increases for the case of metal box cover and similarly for the case of RF-shield box cover, as expected. This allows us to conclude the metal cover reduces the accuracy more in comparison with the wood cover; meaning that large differences are expected between true locations and UWB measured locations in the presence of metal.

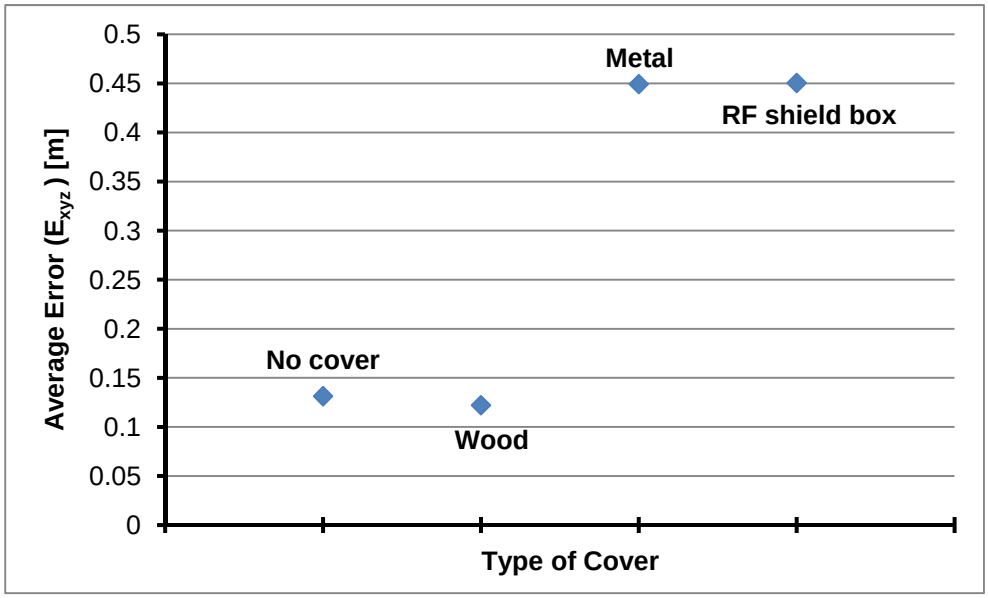

Figure 15: Average errors (E_{xyz}) associated with each cover (calculated for all readings).

The effect of location on average error (or accuracy of the system) is illustrated in Figure 16. This figure indicates that the accuracy of the system does not change significantly at the different points for the no cover and wood box cover configurations, but the average error associated with the other two covers (i.e., metal box and RF-shield box) shows larger differences depending on the location; this means that the UWB measured locations are closer to their true locations when they

are tagged in an environment free from metal presence. The detailed effect of location on the system accuracy is addressed further in Chapter 4 and Chapter 5.

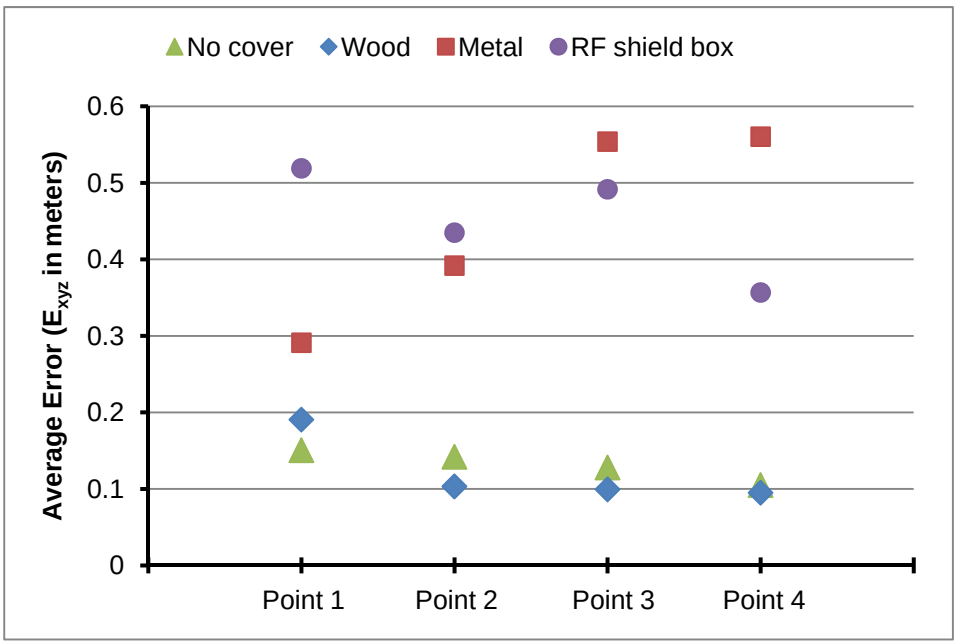

Figure 16: Average error (E_{xyz}) at different locations for different covers.

Figure 17 shows tag to tag variation of the average error for different covers. It is good to mention that all of the tags used in the study were compact tags. The plot indicates that tag 4 has the largest average error for no cover and wood cover; however, there is not a large tag to tag variation for these two covers. For the RF-shield box cover, the average errors for different tags are almost the same but generally it is higher than no cover and wood box. The metal cover has a large tag to tag error variation. Tag 4 is the most accurate and Tag 1 is the least accurate in this group. These observations suggest that, different tags may have varied accuracy in different environments. The discrepancies among different tags accuracies may be related to the tag built-in battery life; thus it is recommended to test the tag

performance before using them in a project to assure data consistency. Since the tag battery is built-in, it is not possible to examine the battery itself. But it is possible and recommended to examine the performance of the tag through the readings accuracy.

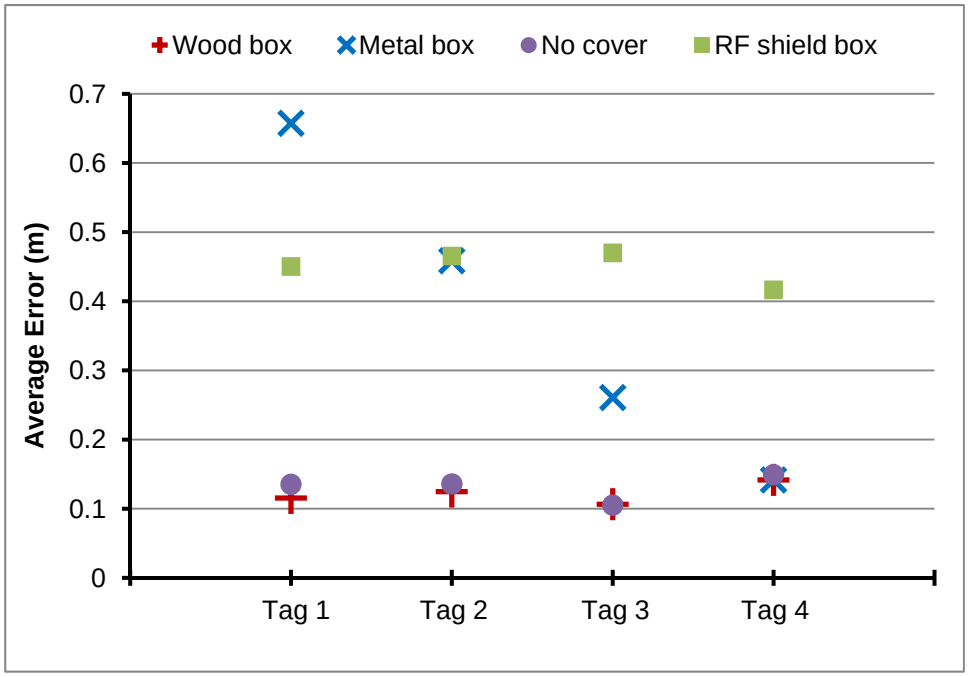

Figure 17: Average error associated with each tag for different covers.

Figures 18 to 20 are the scatter plots of E_y versus E_x for the different cover types. E_x and E_y are calculated from the following formulas:

$$E_x = x - x_t \tag{3.2}$$

$$E_y = y - y_t \tag{3.3}$$

$$E_y = z - z_t \tag{3.4}$$

Since z_t is the same for all four locations, we are not interested in measuring the z values; therefore E_z is not calculated.

Figure 18 shows the scatter plot of E_y vs. E_x when no cover is applied. This figure shows that E_x is always negative, and varies between -0.13 m and -0.048 m; E_y takes both positive and negative values varying from -0.081 m to 0.099 m. Based on the sample error, it can be concluded that there is a systematic error in the negative x direction associated with the no cover configuration.

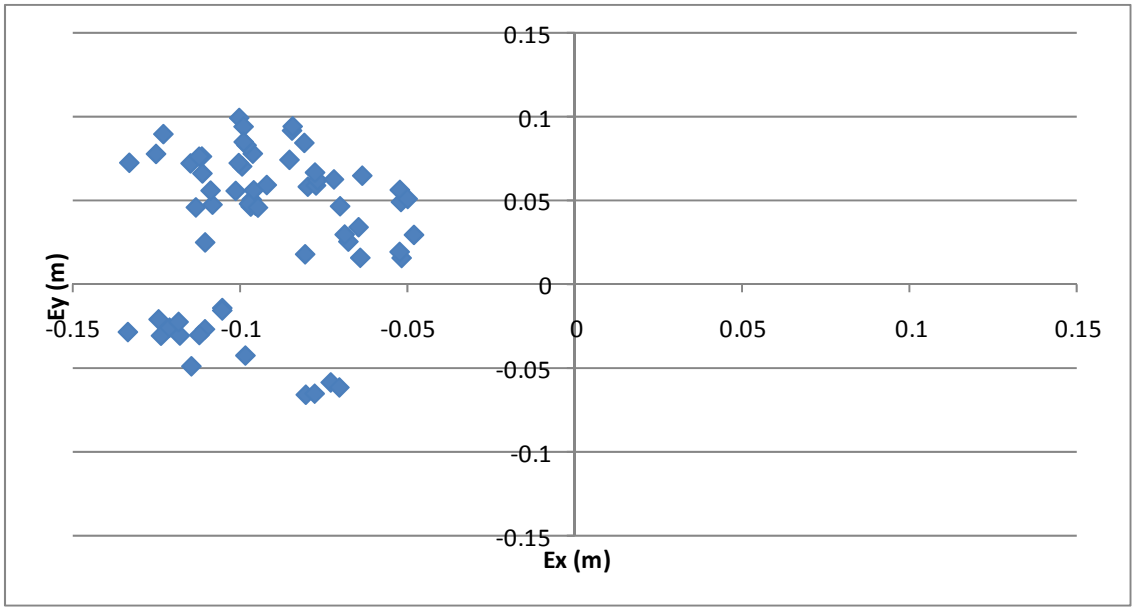

Figure 18: Scatter plot of E_y (m) vs. E_x (m) - without cover.

A scatter plot of E_y vs. E_x for the wood box cover is shown in Figure 19. The plot shows almost similar results to the results for no cover (Fig. 17). E_x is again negative in all samples, and ranges between -0.134 m to -0.021 m. E_y varies from -0.091 m to +0.067 m for different samples. Again, a systematic error in the negative x direction is visible, indicating the system accuracy for the no cover and wood cover condition is similar.

A Scatter plot of E_y vs. E_X for the metal box cover is depicted in Figure 20. Comparing this figure to the no cover case, the average of E_X has moved to the

positive side and varies over a larger range between -0.668 m and 0.765 m. the average of E_y has moved to the positive side and varies from -0.306 m to 0.338 m.

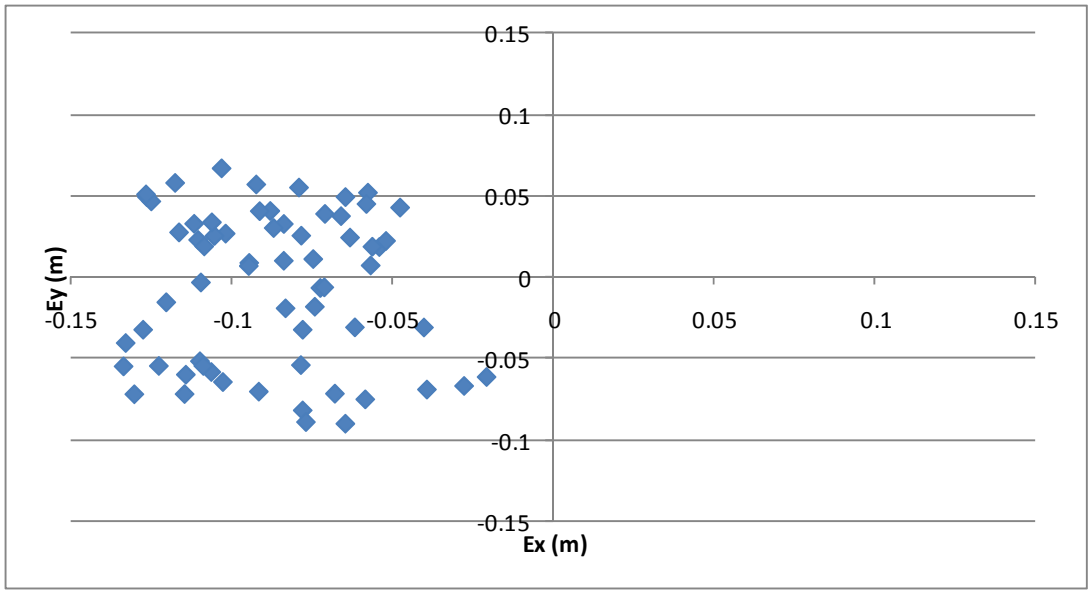

Figure 19: Scatter plot of E_y (m) vs. E_x (m) - wood box.

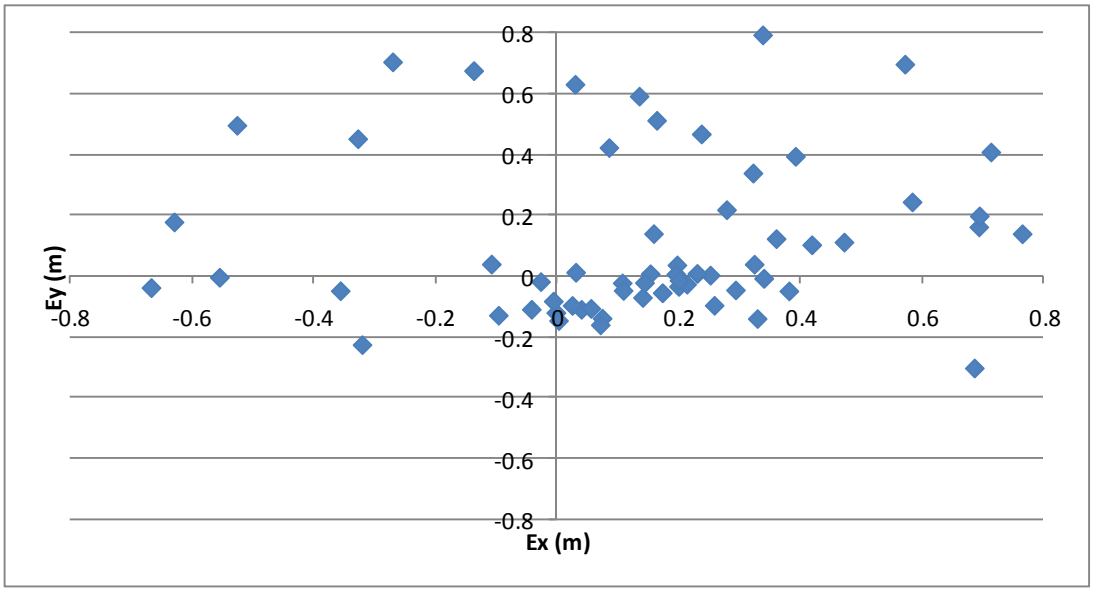

Figure 20: Scatter plot of E_y (m) vs. E_x (m)- metal box.

In Figure 21, the scatter plot of E_y vs. E_X for RF-shield box is depicted. Similar to the metal cover configuration, the average of E_X and E_y moved to the positive sides of both x and y axis and the samples are scattered over a larger range compared to the no cover or wood box cases; E_X ranges from -0.779 m to 0.328 m and E_y ranges from -0.539 m to 0.322 m.

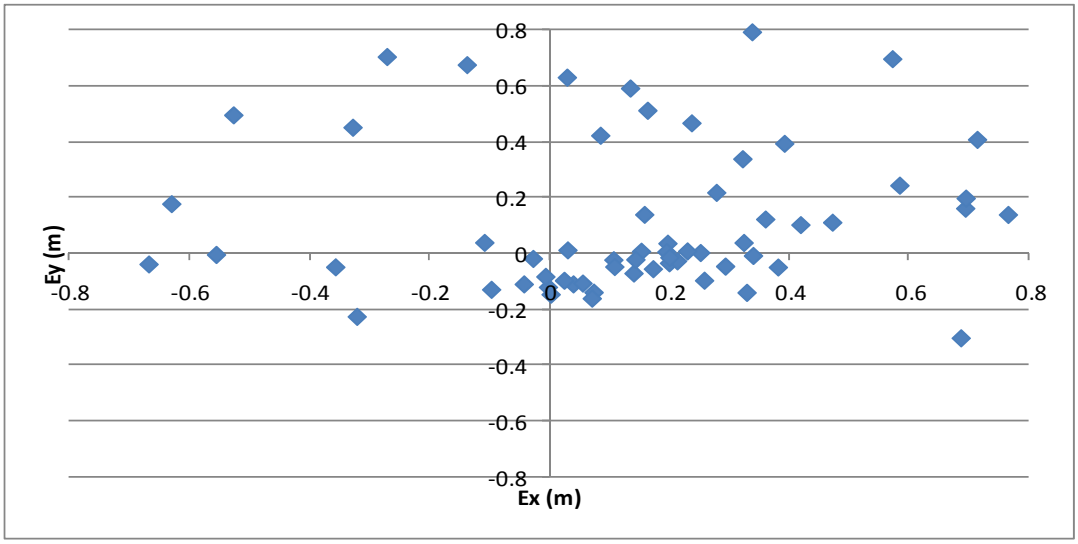

Figure 21: Scatter plot of E_y (m) vs. E_x (m) - RF-shield box.

The differences in x- and y- error for the wood box cover and metal box cover are illustrated in Figure 22. This figure shows that in the presence of the metal box, the readings from the UWB system are more scattered and moves to positive direction of both x and y axis. This means that the errors from the true locations are larger in the presence of the metal box. The scattered data can be interpreted as the multipath effect caused by the metal surface. Since the line of sight of the tag is blocked in metal cover configuration, the UWB signals reflect from the metal and

produce the errors in the measurements. The negative error in both no cover and wood configurations indicates that the systematic error associated with the UWB system has a negative mean.

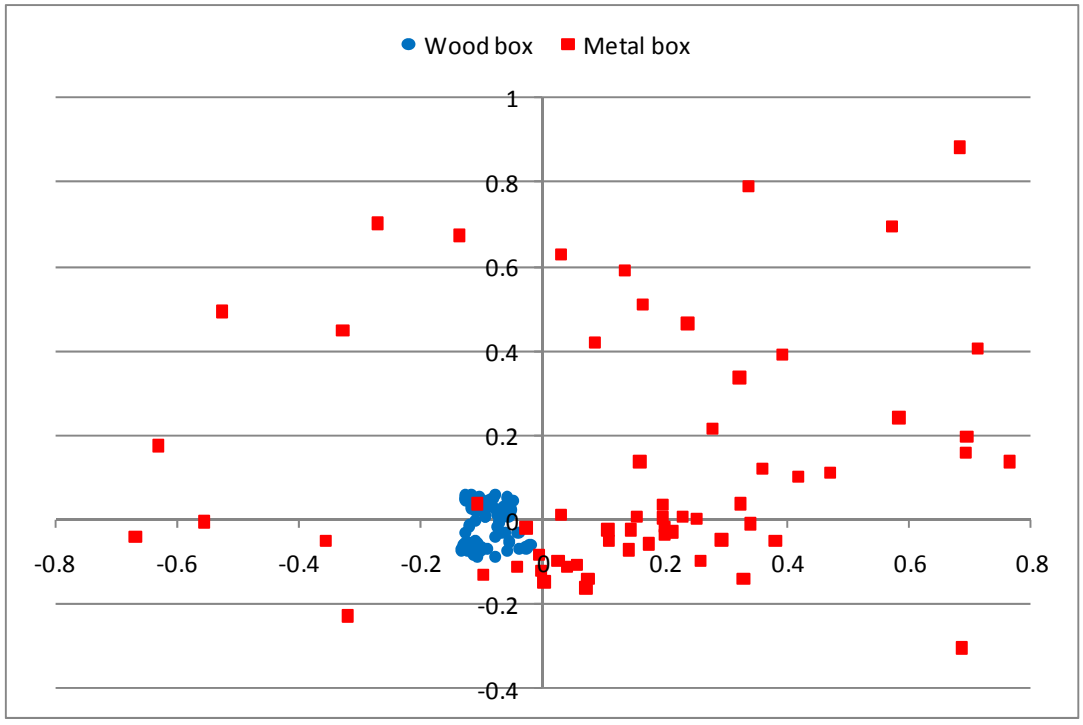

Figure 22: Scatter plot of E_y (m) vs. E_x (m) for wood box and metal box in the same scale.

3.2.1 Statistical Analysis

In statistics, analysis of variance (ANOVA) is a collection of statistical models in which the variance of a particular variable is partitioned into components with different sources of variation (Montgomery, 2001).

For comparing statistical models that have been fit to a data set and to identify the model that best fits the population from which the data were sampled, F-test is usually applied. F-test is any statistical test in which the test statistic has an F-distribution under the null hypothesis (Montgomery, 2001).

Generally, in an F-test, a decomposition of the variability in a collection of data in terms of sums of squares is considered. The test statistic in an F-test is the ratio of two scaled sums of squares reflecting different sources of variability. When the null hypothesis is not true, these sums of squares lead to a greater statistics. If the statistics follow the F-distribution, these sums of squares should be statistically independent (Montgomery, 2001).

In this part of the study, an analysis of variance (ANOVA) has been conducted on the average errors associated with different configurations to find significant factors among the three main factors (i.e., cover, tag, and location). The ANOVA results are presented in Table 10. The formulas used to calculate the ANOVA components are as follows (Montgomery, 2001):

$$S_C = \frac{y_{....}^2}{4 \times 4 \times 4 \times 4} \tag{3.5}$$

$$SS_{tag} = \frac{1}{4 \times 4 \times 4} \sum_{i=1}^{4} y_{i...}^2 - S_c \tag{3.6}$$

$$SS_{\text{cover}} = \frac{1}{4 \times 4 \times 4} \sum_{j=1}^{4} y_{.j..}^2 - S_c \tag{3.7}$$

$$SS_{location} = \frac{1}{4 \times 4 \times 4} \sum_{k=1}^{4} y_{..k.}^2 - S_c \tag{3.8}$$

$$SS_{(tag-\text{cover})} = \frac{1}{4 \times 4} \sum_{i=1}^{4} \sum_{j=1}^{4} y_{ij..}^2 - S_c - SS_{tag} - SS_{\text{cover}} \tag{3.9}$$

$$SS_{(tag-location)} = \frac{1}{4 \times 4} \sum_{i=1}^{4} \sum_{k=1}^{4} y_{i.k.}^2 - S_c - SS_{tag} - SS_{location} \tag{3.10}$$

$$SS_{(cover-location)} = \frac{1}{4\times 4}\sum_{j=1}^{4}\sum_{k=1}^{4} y_{.jk.}^2 - S_c - SS_{cover} - SS_{location} \tag{3.11}$$

$$SS_{(tag-cover-location)} = \frac{1}{4}\sum_{i=1}^{4}\sum_{j=1}^{4}\sum_{k=1}^{4} y_{ijk.}^2 - S_c - SS_{tag} - SS_{cover} - SS_{location} \tag{3.12}$$

$$SS_{subtotal} = \frac{1}{4}\sum_{i=1}^{4}\sum_{j=1}^{4}\sum_{k=1}^{4} y_{ijk.}^2 - S_c \tag{3.13}$$

$$SS_E = SS_T - SS_{subtotal} = \sum_{i=1}^{4}\sum_{j=1}^{4}\sum_{k=1}^{4}\sum_{l=1}^{4} y_{ijkl}^2 - S_C \tag{3.14}$$

A P-value is a measure of how much evidence we have against the null hypothesis. The null hypothesis is usually represents the hypothesis of no change or no effect and is represented by the symbol H_0. The smaller P-value shows more evidence against the null hypothesis.

One way to report a hypothesis result is to state that at a specified level of significance (α), the null hypothesis was or was not rejected. This statement is often inadequate because it cannot be defined how far the computed value of the test statistic is in the rejection region (is that just barely in the rejection region or it is very far into this region). Furthermore, this way of result presentation imposed a predefined level of significance on other users of the information (Montgomery, 2001). To avoid these difficulties, P-value approach has been applied in this part of the study. "The P-value is the probability the test statistic will take on a value that is at least as extreme as the observed value of the statistic when the null hypothesis H_0 is true" (Montgomery, 2001). Therefore, P-value shows the weight of existing evidence against H_0 and enables the decision maker to conclude at any specified level of

significance. In practice, the P-value is defined as the smallest level of significance that would lead to rejection of the null hypothesis H_0. The general rule is that a small P-value is evidence against the null hypothesis while a large P-value means little or no evidence against the null hypothesis.

Table 10: Analysis of Variation (ANOVA) results for E_{xyz} for all data sets (no cover, wood box, metal box, Rf-shield box).

Source	SS	DF	MS	Fo	Fcr	P-Value
A(Tag)	0.41138	3	0.13713	8.04972	2.60490	0.00004
B(Cover)	11.30330	3	3.76777	221.17733	2.60490	0.00000
C(Location)	0.22993	3	0.07664	4.49910	2.60490	0.00447
AB	1.90450	9	0.21161	12.42210	1.87990	0.00000
AC	0.46537	9	0.05171	3.03540	1.87990	0.00204
BC	1.44561	9	0.16062	9.42896	1.87990	0.00000
ABC	0.92613	27	0.03430	2.01356	1.48000	0.00359
Error	3.27073	192	0.01704			
Total	19.95694	255				

As indicated in the ANOVA table, the cover factor is very significant, with a confidence level of almost 100% (1-0.00000=1). This result was expected, as blocking the tag with the RF-shield box or even the metal box was expected to have a significant negative impact on the accuracy of the system. However, the ANOVA analysis also revealed some unexpected and rather unfavorable results. According to the P-values, the tag to tag variability is also significant at almost 100% (1-0.00004=0.99996) level of significance. This unfavorable result indicates that the accuracy of the system is affected by a particular tag that is used in the system, which reduces the reliability and repeatability of the result obtained from any one tag. Another result reveals that the location has also a significant effect on the system accuracy. This is shown in the ANOVA table based on the statistical analysis, but

there is no error pattern related to a special location and the error is completely random. The other unexpected result was the significance of the interaction between the factors. The P-values for the interactions indicate that the interaction plays a significant role in the system accuracy. These interactions need to be analyzed in the future experimental programs in order to investigate their nature. Since it is not investigated in the current study, further investigation is suggested in the future work.

Looking to Figures 20 and 21, it can be seen that, the metal box and the RF-shield box data is more scattered (randomized) than the other two cover types data. Therefore, to better investigate the effect of different factors, we decided to exclude the metal box and the RF-shield box readings and perform ANOVA on the remaining sets of data. The ANOVA results excluding metal box and RF-shield box data sets are presented in Table 11. Having less degree of freedom for covers (it is decreased from 3 to 1), the variation of readings among the covers is also decreased and as a result the effects of tag and location tag are intensified. As you can see, Table 11 illustrates this result by showing the smaller P-values for tag and location in comparison with those values in Table 10. On the other hand, larger P-values for both tag-location (AC) and tag-cover-location (ABC) interactions decrease evidences to reject the null hypothesis (the factors effect is not significant), therefore these two interactions do not significantly impact the accuracy of the system.

Table 11: Analysis of Variation (ANOVA) results for E_{xyz} for data sets excluding metal box and RF-shield box data.

Source	SS	DF	MS	F(observed)	F(critical)	P-Value
A(Tag)	0.02548	3	0.00849	48.34754	2.71140	0.00000
B(Cover)	0.00215	1	0.00215	12.24438	3.95250	0.00071
C(Location)	0.08202	3	0.02734	155.60542	2.71140	0.00000
AB	0.00236	3	0.00079	4.47967	2.71140	0.00548
AC	0.00107	9	0.00012	0.67765	1.99130	0.72726
BC	0.02840	3	0.00947	53.89026	2.71140	0.00000
ABC	0.00149	9	0.00017	0.94254	1.99130	0.49244
Error	0.01687	96	0.00018			
Total	0.15985	127				

3.3 **Summary**

In this chapter, a preliminary study on the performance of a UWB system installed in a lab environment was performed and the effects of different factors such as material, different tags, and tag location on the accuracy of the system were investigated. Considering the average error as the representative of the system accuracy, it has been shown that all aforementioned factors significantly affect the system accuracy. To study the material effect, four types of cover (i.e., no cover, wood box, metal box, and RF-shield box) have been considered and among those metal and RF-shield boxes have the most negative impact on the accuracy of the system. It was interpreted as the effect of multipath signals reflected from the metal surfaces that interfere the UWB system.

Chapter 4

UWB Position Location in an Active Construction Site

In this chapter, the use of a UWB system in a building construction site located on the university of Waterloo campus is discussed. The performance of the system is investigated and the lessons learned from applying the UWB system in a real construction site are shared.

Effective construction management involves real-time decisions involving the progress of specific activities and the location of materials and equipment. A UWB system along with other sources of information in a construction project could provide a more accurate estimation of a construction progress. This is the base of the proposed data fusion model by Shahi (Shahi, 2010). In this model, a fuzzy logic inference system (i.e., multi-sensor data fusion) is used to combine the information from various sources such as a building information model (BIM), 3-D laser scans, schedule information, RFID, and UWB information.

A UWB system can potentially be applied to update the progress of tasks consisted of different activities (Shahi, 2010). Pipe installation tracking could be considered as one application since it consists of various activities such as: delivery to

lay-down yard, delivery to installation site, installation, welding/fitting, and inspection. The model for progress tracking of a piping project with a UWB system was proposed by Shahi (Shahi, 2010). Based on the proposed model, the welder is equipped with a UWB tag which is identified by its distinct barcode. As soon as the welding process on a piece of pipe is completed the welder would place the tag on the pipe and the system will monitor the tag location which indicates that the welding phase is completed. The same technique is applicable for pipe inspection. The number of required tags will increase as the pipe numbers increase. But, the indicator tags could be reused after a short cycle time (e.g. 10-15 seconds). This way the number of required tags at any time is manageable and only one or two tags would be enough for each welder or inspector. Some of the collected data in this phase of the research will be used as one component of the information which is required for the proposed data fusion system by Shahi (Shahi, 2010).

In the following section, the installation challenges faced with are addressed. Furthermore, the effect of construction progress and changes to the built environment on the performance of the installed UWB system are discussed.

4.1 System Setup

A UWB system including four receivers was implemented in the E6 building under construction on the University of Waterloo campus. The goal of this part of the study was to investigate the performance of a UWB system in a real construction project facing different and evolving conditions on site. Four receivers were installed on the fifth floor service corridor of the building, where several types of pipes,

ductwork and other equipment were to be installed. The service corridor is an enclosed passageway where lots of cables and several types of duct and pipe are going to be installed there. The fifth floor service corridor were chosen for this study, since it gets too busy when the cables and the pieces of pipe and ducts from four lower floors, all merge together on the fifth floor. Therefore tagging different pieces of pipes and ducts simplify progress tracking of the service corridor. This part of the data will be used by other researchers at University of Waterloo. The plan view for the corridor, the position of investigated points and the location of the UWB receivers, are depicted in Figure 23.

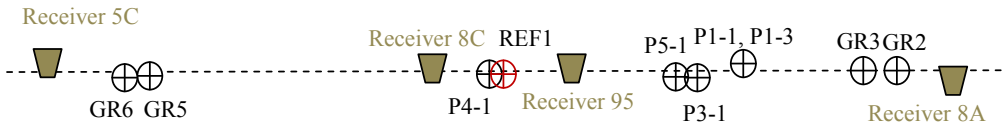

Figure 23: The position of the receivers and the investigated points in the 5th floor service corridor (The GR points are located on the floor and the P points are located on the pipes).

The UWB receivers were mounted on the ceiling. In Figure 24 the 5th floor service corridor where the data was collected, is shown. This figure clarifies that the receivers are installed approximately in the middle of the corridor. This arrangement was necessary since when the sensors were installed, no walls had been erected around the corridor area, and because a large amount of pipe and ductworks to be installed on each side of the corridor, increasing the risk of the sensors being damaged.

Figure 24: The service corridor in E6 construction site in the University of Waterloo (the UWB receivers in the picture are circled).

Figures 25 and 26, respectively, show the service corridor environment at the time of the sensor installation and at the end of the data collection phase. Although the preliminary linear installation arrangement does not follow the recommended sensor configuration, it was the only available option in this particular application. The challenges associated with this decision are addressed later in this chapter.

Figure 25: The service corridor at the beginning of the study (walls not installed).

Figure 26: Service corridor at the end of the study

4.2 Data Collection

The data collection phase was started in September 2010. During the three-month period of data collection, different measurement points located both on the floor and on pipes were located using the installed UWB positioning system. The points were distributed along the service corridor and represent the area under the UWB system coverage. Based on the error given by Equation (3.1), the accuracy of the system for different dates during the data collection period for different sections of the corridor was investigated. Based on this information the conclusions about the system performance are made. Since

4.3 Installation Challenges

The research group faced different challenges during installation and operation of the UWB positioning system in this field experiment. The most significant challenges and the suggested solutions are discussed below.

4.3.1 Layout of the Receivers

As mentioned earlier, the AOA and TDOA principles are both used by the UWB system to compute a tag position. The optimum layout to apply these principles is to have a rectangular configuration for the receivers. It is also advantageous to consider the future changes in construction site environment to avoid any system shut down and to maintain the system for a longer period.

4.3.2 System Power Supply

Power shut down in a construction site due to different reasons is possible. When the UWB system is booted up and the receivers are connected, system calibration is necessary in order to introduce the receiver positions to the system. Calibration enables the system to compute the tags location correctly. This step is very important, since the calibration process affects the accuracy of the readings obtained from the system. In other words, an accurate UWB positioning system is only possible if the calibration was performed accurately. Knowing that the receivers are fed through a POE switch plugged into an electrical power source, it is more advantageous to have a stable, reliable power supply for the system separate than the power supply used for construction which may be prone to shut down. This will avoid repeated calibration, and the readings will be more consistent.

4.3.3 Receiver Connection

The receivers have to be connected to each other to receive timing data which enables them to know their positions based to the master receiver position. The common type of connection is CAT5 cables. When the construction site is congested and the distances between receivers are too long, wireless connection could be advantageous.

4.3.4 Cabling problems

If cabling was chosen as the connection method, it is preferable to use manufactured CAT-5e cables with factory installed connectors. Non-manufactured cables are usually problematic and do not function properly. Testing the cables with a cable qualification tester device before plugging them in the sensors helps to diagnose

connection- related problems. A cable qualification tester and the transmitter are depicted in Figure 27.

The tester can diagnose cabling errors, and can also identify problematic switch ports. This is particularly useful when the cables are long and it is hard to find the end of each cable in a batch of cable. A transmitter attaches to one end of the cable and on the other end the cable plugs into the tester and the information is displayed on the screen. In our case, for the CAT-5e cables the tester shows the wrong connected switch port by its number. In this research study, the cable tester was used to identify and correct cable layout and switch port connection problems.

There is an accessory available in the market which is suitable to use in environments where cabling is difficult to run or its cost is very high. This accessory is a network and timing combiner. In environments requiring long cable runs for system installation, the combiner reduces the number of long cable runs by combining network, power and timing signals into a single shielded cable (Product fact sheets). This accessory is shown in Figure 28.

Figure 27: A cable qualification tester and the transmitter.

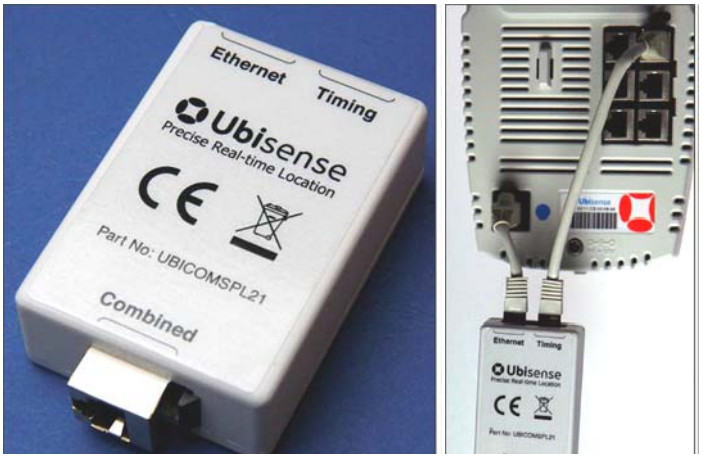

Figure 28: Network and timing combiner accessory.

4.3.5 **Data Acquisition Software:**

Data acquisition software for this research named "Location Engine Configuration" was provided with the Ubisense® Company. As mentioned earlier in Chapter 2, before running the Ubisense® software each receiver needs to get an IP address through a server which supports Dynamic Host Configuration Protocol (DHCP). Windows vista which was installed on the laptop used to collect data was not compatible with the installed DHCP server. To compensate the problem a hardware router was used between the laptop and the POE switch. The router works as a DHCP server and assigns a unique IP address to each of the receivers on the network.

4.4 **Results**

As mentioned earlier, there are two types of measurement points investigated in this section: points located on the floor with $z = 0$, and points located on pipes with

$z \neq 0$. 40 readings on each point were recorded and the errors (E_x, E_y, E_z, E_{xyz}, E_{xy}) associated with 40 readings is calculated using Equations (3.1) to (3.4) and Equation (4.1). For the points located on the floor, elevation read by the UWB system is not important and two-dimensional error (E_{xy}) is considered as an indication of the system accuracy. E_{xy} is calculated by:

$$E_{xy} = \sqrt{(x - x_t)^2 + (y - y_t)^2} \tag{4.1}$$

Then the total average error is calculated by averaging these 40 errors. The results are shown in Tables 12 and 13. Number of days that the UWB reading were recorded for that special point is also reported in Tables 12 and 13. As mentioned earlier, the location of the points is illustrated in Figure 23.

Table 12: Average errors (m) & associated standard deviations (m) calculated for points located on the floor (z=0).

	GR 2	GR 3	GR 5	GR 6
# of days	9	7	9	7
Ave.E_x	0.039	-0.010	0.465	0.502
Stdev.E_x	0.039	0.067	0.173	0.215
Ave.E_y	0.438	0.214	0.022	-0.243
Stdev.E_y	0.095	0.109	0.168	0.292
Ave.E_{xy}	0.442	0.234	0.513	0.640
Stdev.E_{xy}	0.091	0.094	0.080	0.131

Table 13: Average errors (*m*) & associated standard deviations (*m*) calculated for points located in height ($z \neq 0$).

	P 4-1	P 5-1	P 6-1	P 1-1	P 1-3	P 3-1
# of days	4	4	4	3	3	3
Ave.E_x	-0.041	0.045	0.019	0.134	0.067	0.108
Stdev.E_x	0.019	0.023	0.139	0.134	0.072	0.050
Ave.E_y	-0.025	-0.122	-0.134	-0.034	0.199	0.348
Stdev.E_y	0.124	0.237	0.756	0.110	0.125	0.126
Ave.Ez	0.225	0.309	-0.087	-0.193	-0.507	-0.663
Stdev.Ez	0.246	0.151	0.417	0.425	0.325	0.424
Ave.E_{xyz}	0.324	0.405	0.703	0.375	0.586	0.806
Stdev.E_{xyz}	0.081	0.102	0.375	0.083	0.250	0.100
Ave.E_{xy}	0.117	0.226	0.613	0.159	0.586	0.372
Stdev.E_{xy}	0.023	0.106	0.339	0.265	0.250	0.289

Table 14: Total average errors (E_{xyz}, E_{xy}) for two different data sets (points located on the floor & points located on the pipes).

	Points located on the floor (GR points)	Points located on the pipes (pipe points)
Total Ave. E_{xyz}	-	0.533
Total Ave. E_{xy}	0.457	0.346

Total average errors (E_{xy}) for points located on the floor and on the pipes are presented in Tables 14. Total average error (E_{xyz}) for the pipe points is 53 *cm*. Table 14 also shows that the total average error (E_{xy}) for points located on the floor is larger (about 11 *cm*) in comparison with the total average error (E_{xy}) for the points located on the pipes. This indicates that the UWB system accuracy is higher in cases that the reading points are not located on the floor. This difference in the system accuracy might be a result of improved line of sight. The points which are located on the floor were surrounded by metallic hand rails that reflect strong multi-path signals that

interfere with the system decreasing the accuracy of the UWB system. The points located on the pipes may be less affected by the hand rails.

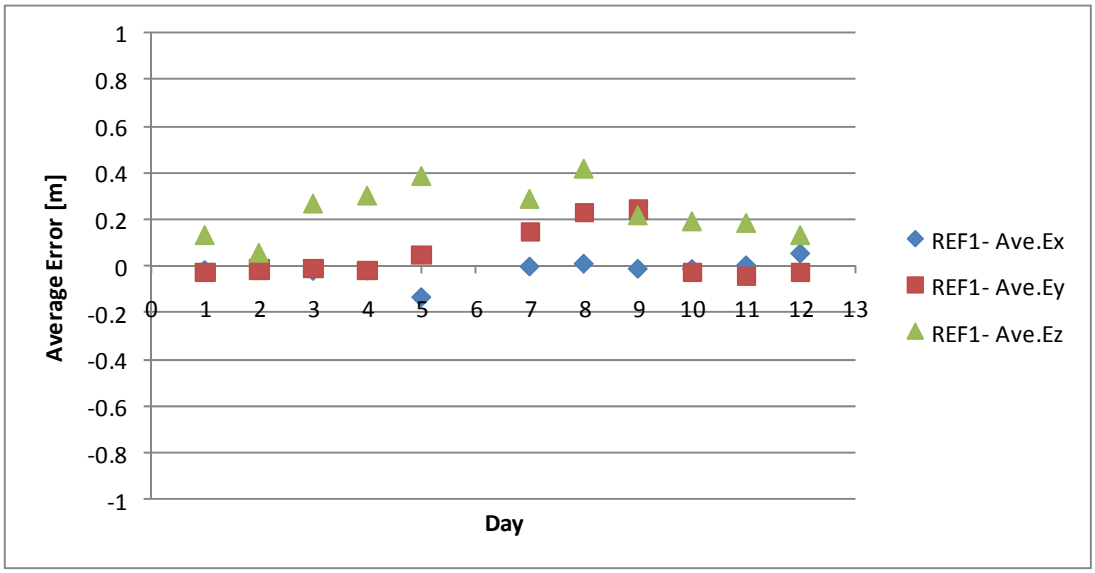

Figure 29: Average error in *x*, *y*, and *z* direction (*m*) over the duration of the experiment for REF1 point based on which the system was calibrated.

Figure 29 depicts the errors associated with the calibration point readings over the duration of the experiment. The calibration point was a fixed point in the middle of the service corridor and the timing data received from the tag located on this point enables the system to calculate the receivers position and estimate any tag location within the covered area. Figure 29 shows that for the calibration point, error in z direction is higher than errors in x and y directions. It also shows in some days the calibration error is higher. This might have happened because of changes in the environment that can affect the system accuracy. E_x is always lower than $0.1m$ except on day five. E_y is increasing between day five and day nine; this increase may be caused by changes made in the environment (e.g., huge pipe and ducts were installed in the corridor during this period). For instance, the presence of large pieces of

metals, pipes or some obstacles may have an impact on the system accuracy. Figure 29 also shows that E_z for the calibration point is almost always greater than E_x and $E_{y,}$ which may be caused by distance between the calibration point and the receivers (the calibration point was located on the floor) or the receiver configuration in a primarily linear arrangement. Another reason for y and z (particularly z) directions could be that all receivers were installed at exact same height (z) and almost the same y, so the location estimation algorithms may not have worked very well in those two directions. The receivers were distributed on the x-axis, which could have caused the good results in that axis.

In the points located on the floor (Table 12), GR3 has the lowest and GR6 has the highest two-dimensional error (i.e., E_{xy}).

The location of points GR5 and GR6 is shown in Figure 23. A reason for this dramatic difference in the average error readings for these points might be related to their position with respect to the receivers as this may result in line of sight signals with different quality. Furthermore, it might be caused by local interferences or the configuration of adjacent interferes in the environment for these two points which are located far from each other. The error components for GR3 and GR6 are shown in Figures 30 and 31.

Since the points in Table 13 are on pipes $(z \neq 0)$, the elevation must be considered. Thus, three dimensional errors given by Equation (3.1) are considered as a measure of the system accuracy. Based on this criterion, P4-1 has the best and P1-3 has the poorest UWB readings. This again might be caused by the difference in the receiver line of sight for the two points, and the different distribution of the adjacent

interferences. The errors associated with these two points on different days are depicted in Figures 32 and 33.

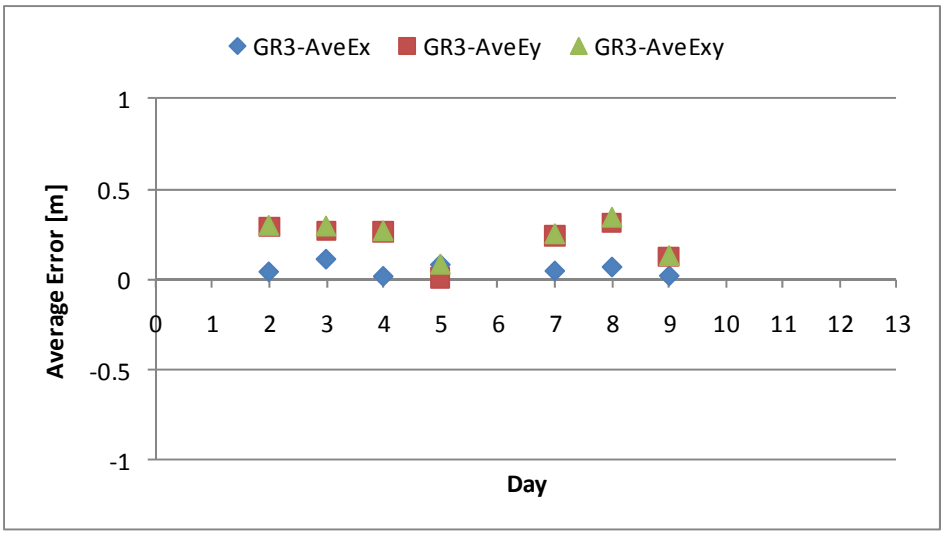

Figure 30: Average errors (E_x, E_y, and E_{xy}) (m) for GR3 on different days.

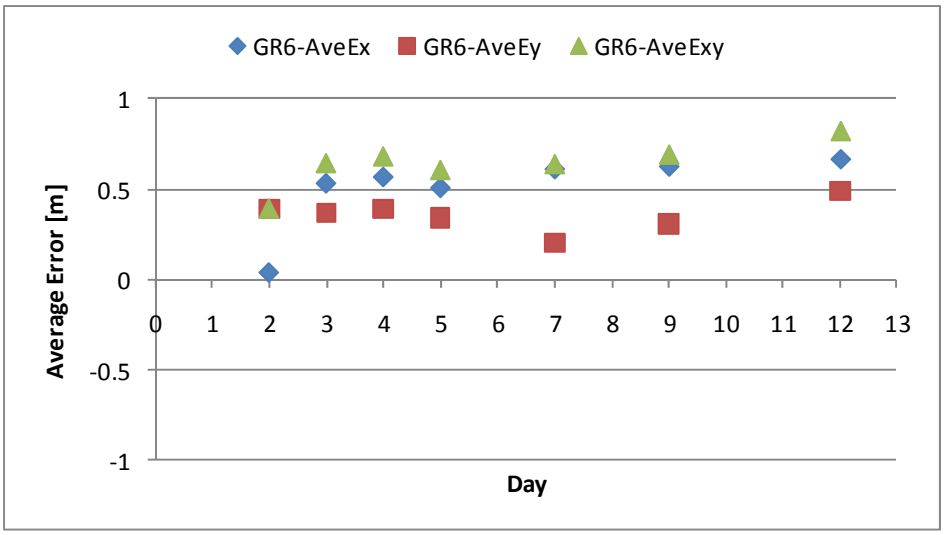

Figure 31: Average errors (E_x, E_y, E_{xy}) (m) for GR6 on different days.

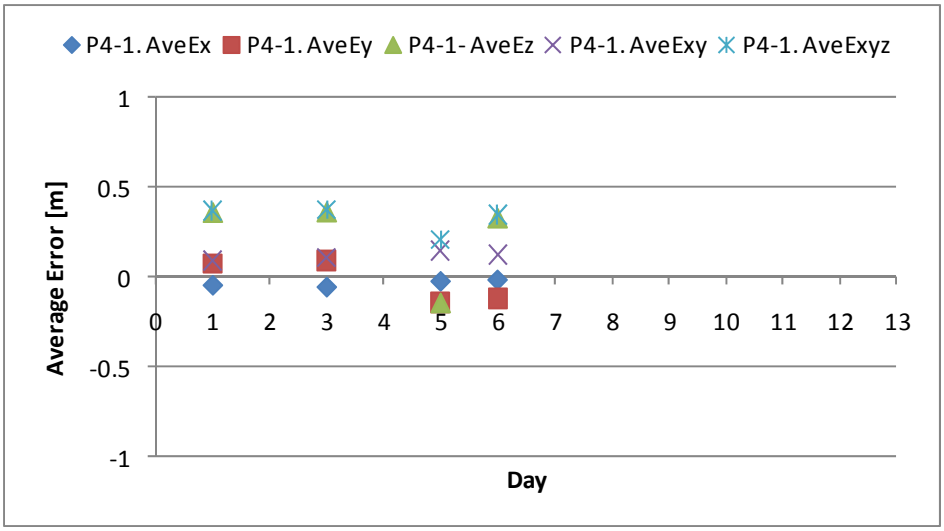

Figure 32: Average errors (E_x, E_y, E_z, E_{xy}, and E_{xyz}) (m) for P4-1 on different days.

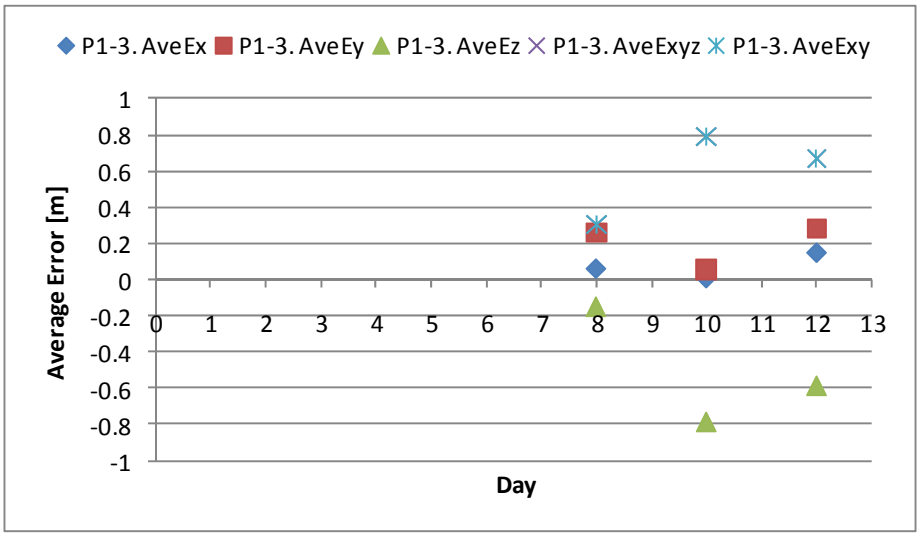

Figure 33: Average errors (E_x, E_y, E_z, E_{xyz}, and E_{xy}) (m) for P1-3 on different days.

4.5 Summary

In this chapter, the application of the UWB positioning system in a real construction site was investigated. Four receivers were installed on the fifth floor

service corridor of a building under construction where several pieces of pipes and other equipment were to be installed. Different challenges associated with installing a UWB system in a construction environment and some recommendations have been addressed. The data was collected during a three month period (Oct 2010-Dec 2010) to monitor the variations in the UWB system performance as well as the progress of the construction environment. The collected data shows that the tag readings for the points located on pipes above the floor level are more accurate (i.e., average error is lower) in comparison with the readings of the points located on the floor; this clear difference in the system accuracy might be a result of improved receiver line of sight. In addition, the points located on the floor were surrounded by metallic hand rails which reflect strong multi-path signals that interfere with the system, decreasing the accuracy of the UWB system.

Chapter 5

Application of UWB Technology in an Automated Safety System

In this chapter the employment of UWB position location systems in safety applications is discussed. In the first phase, error modeling for a UWB system installed in the structure lab at the University of Waterloo was performed. In the second phase, a UWB alarm system was designed to warn the workers when they get close to a predefined hazardous zone. An analysis was conducted to determine an algorithm for the alarm process.

5.1 The Proposed Automated Safety System

As mentioned in the Chapter 2, one application of the UWB positioning system is in safety applications. For this purpose, equipment and workers can be tagged and their locations and movements can be tracked. Moreover, an alarm system can be designed to monitor the safety distance between a worker and equipment, or between a worker and a hazardous zone. Whenever the worker passes this safety zone the system alarms and the worker or the equipment operator will be notified of the hazardous situation. A real-time data collection system is required for this

application. The fast update rate of the UWB system makes this system an excellent potential solution for this application.

In this chapter, an automated safety system using the UWB technology is introduced and its reliability is evaluated. In this system, the position of any tagged object is monitored using the real-time UWB data acquisition system introduced in previous chapters. The system alarms whenever a moving tagged object enters a predefined caution area nearby the hazardous zone. This caution area is called the caution zone. Figure 34 demonstrates the zones defined for the proposed safety system. The hazardous zone is the area in which a hazard might happen for the tag carrier (e.g., worker). The system is intended to prevent the tag career from entering this zone by alarming the worker ahead when he/she is still in the caution zone. A uniform movement for the tag carrier within the area is considered. As it is observed in Figure 34, the caution zone is considered to be a rectangular area located adjacent to the hazardous zone. In general, however, the geometry of the caution zone can be designed appropriately according to the characteristics of the environment, the tag carrier movement, and the risk associated with the danger. As illustrated in Figure 34, a vicinity zone is also defined in the vicinity of the caution zone with the same area as the caution zone.

As discussed in the previous chapters, the locating process using the UWB positioning system involves systematic errors depending on the tag position in the covered area. Therefore, error modeling is conducted in order to precisely model the behaviour of the positioning process in the automated safety system. This model can be employed to design an optimum algorithm required for alarming process. In order to characterize the optimality of this algorithm, a proper performance criterion should

be defined. For the proposed safety system, some performance metrics are considered such as false alarm rate, detection rate and miss rate.

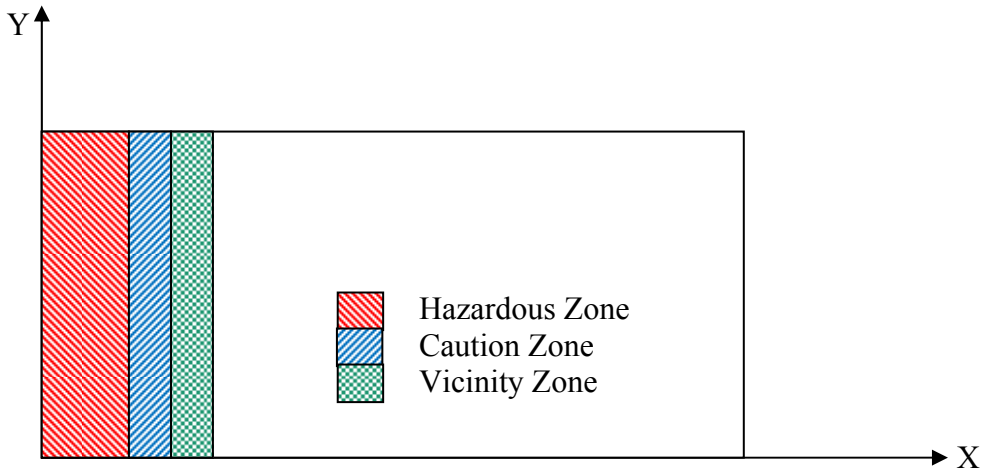

Figure 34: Different zones and their boundaries defined to calculate the reliability of UWB system in safety applications.

A false alarm event happens when the system falsely alarms although the tag has not entered to the caution zone and is still within the vicinity zone. This is not desirable since it decreases the reliability of the safety system by reducing the workers' sensitivity to the warning system as they get used to hearing the false alarm frequently. On the other hand, a detection event happens when the system successfully alarms while the tag is within the caution zone. Otherwise miss event happens, i.e., the system fails to alarm although the tag has entered to the caution zone.

Note that the false alarms usually happen when the tag carrier is within the vicinity zone. In fact, the probability of the false alarm is extremely rare when the tag has not entered the vicinity zone. Therefore, the false alarm rate is defined as the conditional probability of the false alarm given that the tag is within the defined

vicinity zone rather than the whole remaining area in the safe side of the covered environment. Otherwise, the level of the false alarm rate might be underestimated as the far regions with very rare false alarm probability average out the overall false alarm rate. Therefore, using this conditional definition, a better judgment about the level of the false alarm rate can be made compared to the level of the miss rate. For this reason, the area of the vicinity zone is assumed to be the same as the area of the caution zone. As mentioned earlier, the size of the caution zone can be designed appropriately according to the characteristics of the environment, the tag carrier movement, and the risk associated with the danger.

5.2 System Setup

The UWB system applied in this phase of the study consists of four receivers which are mounted on the surrounding walls looking downward to the work area to be covered. The receivers are installed in a rectangular configuration which is recommended by the Ubisense® Company and they are connected in a star topology. Figures 35 and 36 show the mounted UWB receivers in red circles. Figure 37 depicts the plan of the area under study, the location of the receivers, and the master sensor to which the other sensors are connected. The hatched area in Figure 37 depicts the area with permanent obstacles that is not investigated in the study. One four-port POE switch, one compact tag, and one router are the other components of the system as well as CAT-5e cables.

Figure 35: The structure lab area with two of the receivers shown.

Figure 36: The alternative view of the structure lab area with the other two receivers shown.

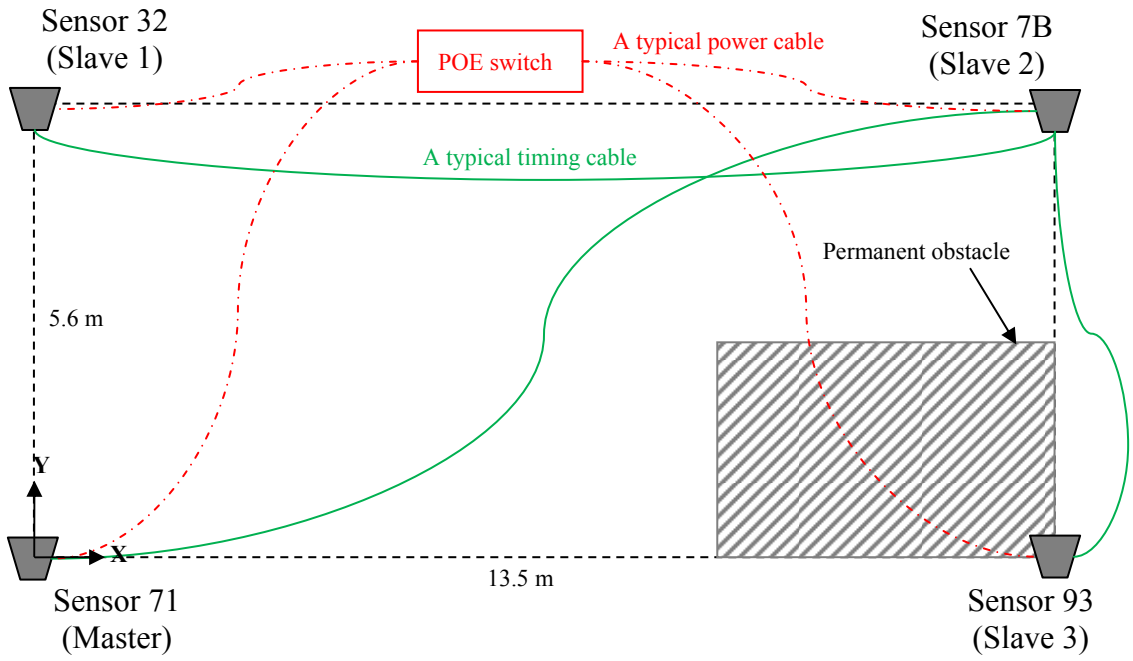

Figure 37: Plan of the study area in the construction lab showing the position of the receivers.

5.3 Error Modeling

In this phase, the error modeling of the UWB system implemented in the lab environment is presented. In Chapter 3, we showed that the system error characteristics vary by location; therefore in this chapter we divide the area into many subdivisions and study the error behaviour of the system at each subdivision in order to model the location-dependency of the system behaviour. For this purpose, a grid size of 30 *cm* was selected for each subdivision. The selected grid size is small enough such that the error behaviour in a single grid can be well approximated by its behaviour at the center point of the gird. Therefore, more than 500 observations were recorded at the center of each grid to model the error behaviour of the system. Note

that the true locations of the grid center points were determined using the total station surveying equipment. The tag which the system intended to calculate its coordinates was always mounted on a pole with 1.7 *m* height (in order to have a better line of sight to the receivers). Since the proposed system is intended to track worker movement within an area, it is not necessary to track the height of the moving tag. Thus, only the system error in the two azimuthal directions as given by Equations (3.2) and (3.3) was considered. Therefore, using these two equations and given (x_t, y_t) at each center point, the statistical behaviour of the error for each grid can be estimated. Having error samples for each point, the error distribution can be statistically described given the true coordinate of that point as $P(x \mid x_t)$ (which means the probability of happening x (observed by the system) if the true location is given as x_t.

Our investigations show that the statistics of the individual error parameters can be well described by Normal distribution. This is justified in Figures 38 and 39 in which the fitted Normal distribution is shown for two sample data sets (each set includes 500 recorded measurements of a single tag on one point). The points can be selected from different parts of the coverage area. 500 coordinate measurements from the UWB system were recorded. Each measurement was compared to the true location of that point read by total station equipment. 500 errors in each direction (x,y) were calculated using Equations (3.2) and (3.3). The average and standard deviation of 500 calculated errors are considered as the mean and standard deviation of the distribution. From these figures, it is clear that the fitted Normal distribution well describes the statistics of the corresponding error samples with different values

of mean (μ) and standard deviation (σ). These mean and standard deviation values were calculated from the UWB system measurements.

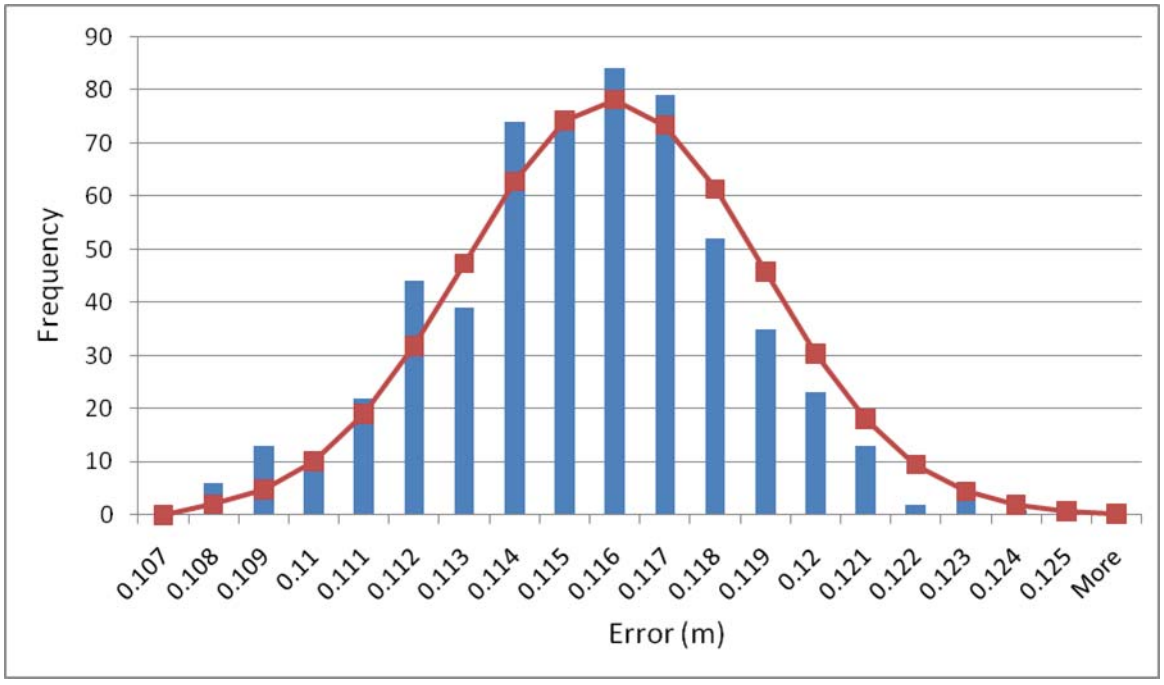

Figure 38: Fitted Normal distribution for E_x at (x=10.18, y=4.9) with μ=0.116, σ= 0.003.

Figure 40 illustrates the average error associated with the center point of the grids in both x and y directions using geometric vectors. The figure shows that the system average error at most of the points is mild except some boundary points which suffer from higher levels of error. Furthermore, the average error magnitude and direction appears to be highly dependent on the location of the tag. Note that the magnitude of the average error at each point shows the level of the systematic error of the system.

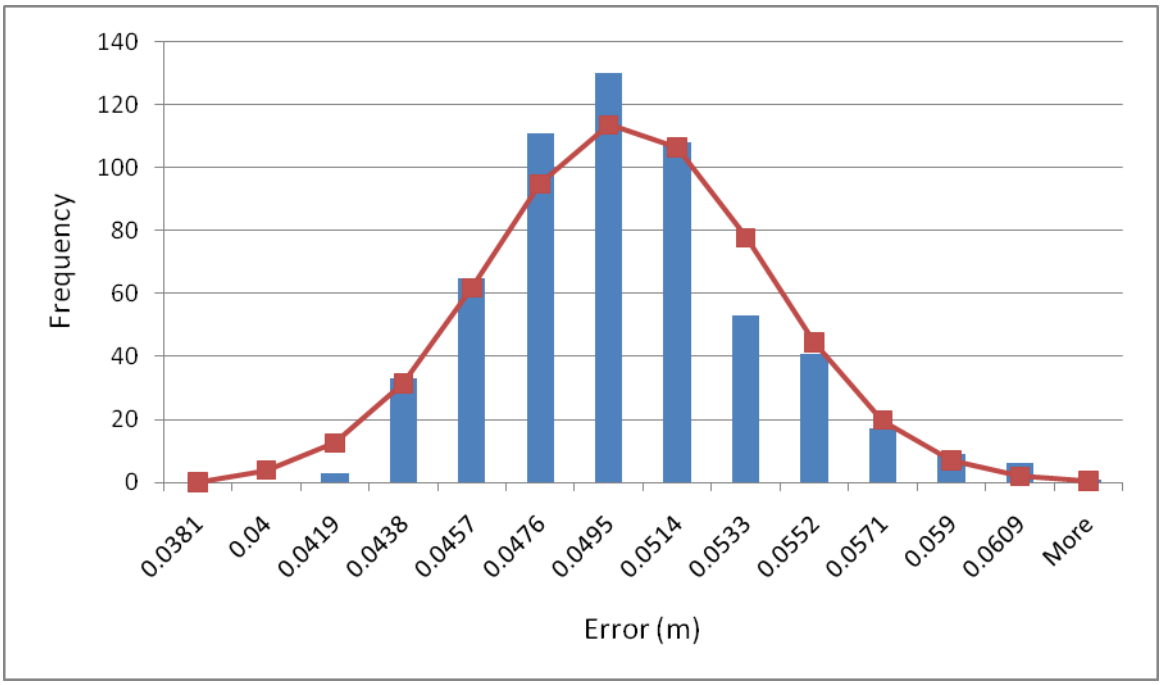

Figure 39: Fitted Normal distribution for E_y at (x=10.18, y=4.9) with μ=0.049, σ= 0.004.

Therefore, having the systematic error as a function of location allows for the compensation of the error in future readings from the UWB system. Specifically, the estimated systematic error at a grid point can be subtracted from the future UWB measurements within the grid.

Comparing the performance of the current UWB system setup with the results of the previous chapter where the UWB sensors were deployed in an in-line configuration, much lower error levels are observed for the current rectangular deployment. This illustrates that the receiver configuration plays a critical role in the performance of the UWB system.

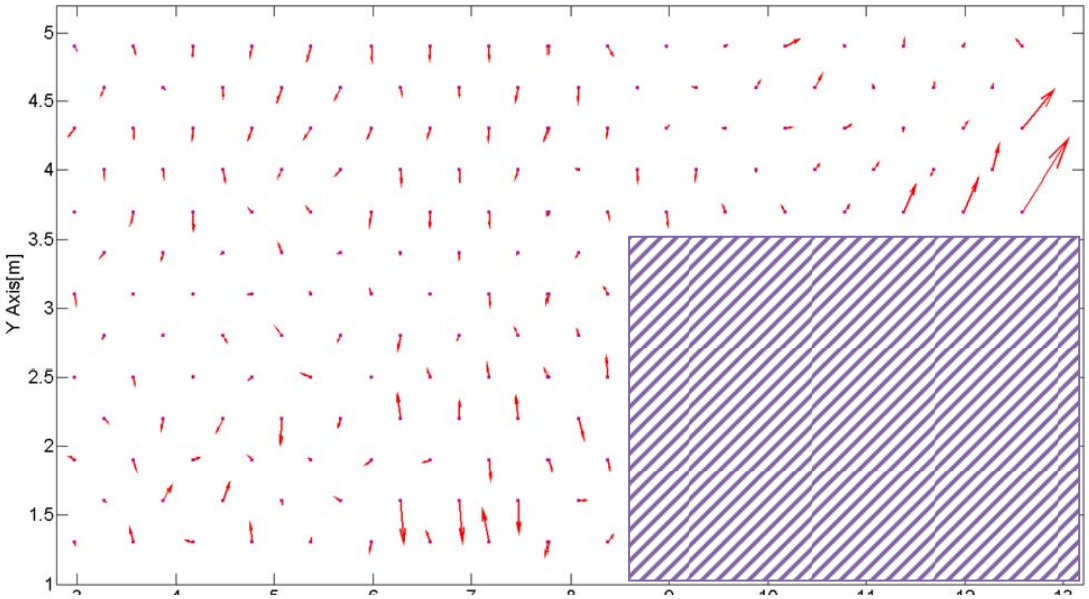

Figure 40: Calculated error vectors (E_{xy}) for different grids.

The variation of the standard deviation of E_{xy} is shown in Figure 41. It can be observed that although for some locations in the area the standard deviation of the error becomes as high as 10 *cm*, it is less than 1 *cm* in the majority of the covered area which shows the reliability of the position location system. Furthermore, assuming that the average error depicted in Figure 40 is estimated and compensated, the performance of the positioning system is significantly improved. The error standard deviation depends on the system characteristics and it cannot be compensated. Therefore, it would be the only source of error.

The average of the error vectors magnitudes over the whole covered area is 8.9 *cm*. As mentioned earlier, some of the boundary regions that occupies less than 5% of the covered area, experience very high error magnitudes and skew this average value. Excluding these high error magnitudes, the average of the error vectors magnitudes over the remaining 95% of covered area is obtained as 5.6 *cm.*

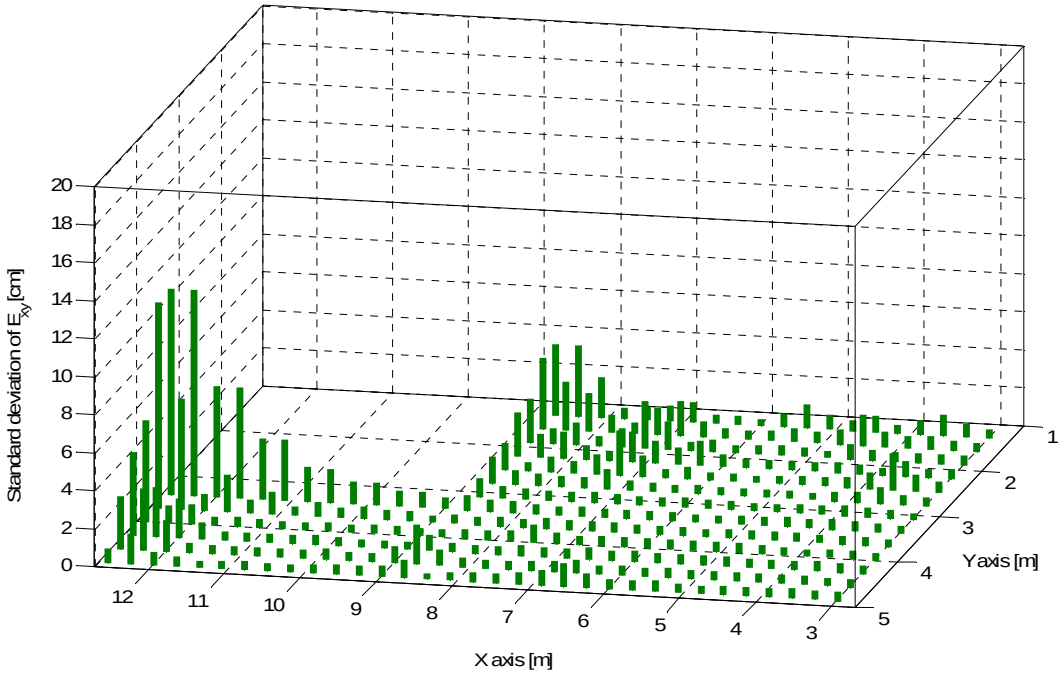

Figure 41: The variation of the standard deviation of E_{xy} over the covered area.

Figure 42 illustrates the contour map of the average error magnitude variation over the covered area. This plot provides a better sense of the continuous variation of the average error magnitude rather than discrete representation given by Figure 40. We can observe many local minima and maxima of the average error magnitude distributed over the area. These extreme variations can be described by the presence of obstacles/interferers in those local regions. In addition, the density of the contour lines demonstrates the rate of the error magnitude variation. For example in the top left quarter, a much lower density of the contour lines can be observed. This shows that this area the average error magnitude does not strongly depend on the tag location. This information can be utilized to further improve the error modeling of the system. In fact the grid size can be modified and redefined adaptively based on the rate of average error variation. This modification can be performed by keeping the

same data samples in the regions with loose contour lines and collecting more data samples within the regions with denser contour lines. This is not performed in this research but it is suggested for the future work.

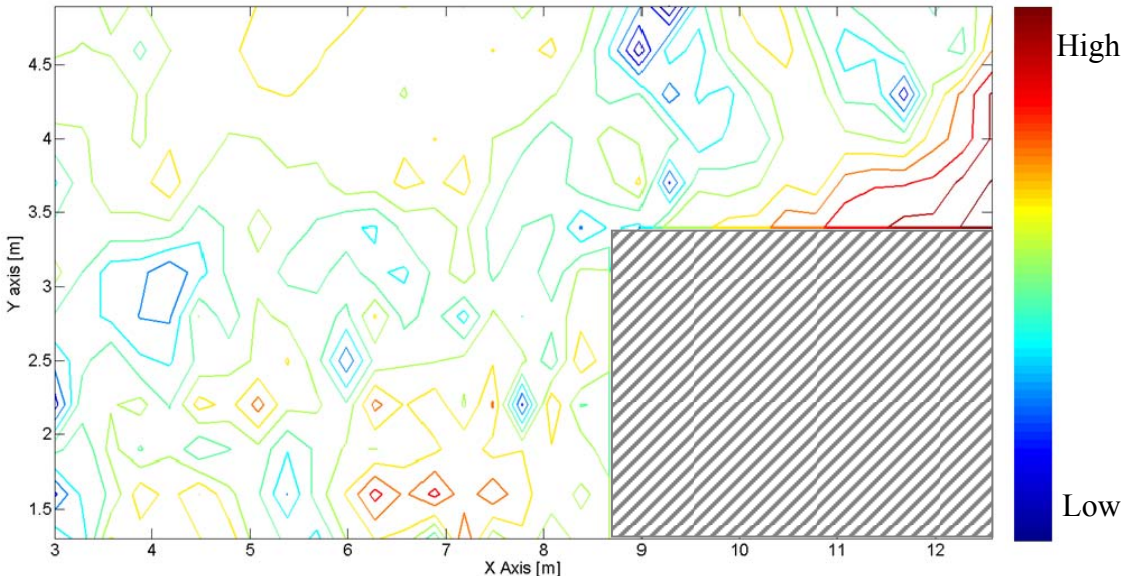

Figure 42 : Contour lines of the average error (E_{xy}).

5.4 Statistical Analysis

In this phase of the study, a statistical analysis was conducted to design the optimum algorithm for the alarm process. For this purpose, a binary hypothesis-testing problem is defined and the optimum solution is presented. Two possible hypotheses of H_0 and H_1 are considered. These hypotheses are characterized by the two probability distributions P_0 and P_1 as follows:

$$\begin{cases} H_0 : X \sim P_0 \\ H_1 : X \sim P_1 \end{cases} \tag{5.1}$$

where the notation $X \sim P$ denotes that the random parameter X has probability distribution of P. The hypotheses H_0 and H_1 are sometimes referred to as the null and alternative hypotheses, respectively. A decision rule (or hypothesis test) δ for H_0 versus H_1 is any partition of the observation set Γ into sets Γ_1 and Γ_0 such that we choose H_j when $x \in \Gamma_j$ for $j = 0$ or 1 where x is any realization of the random parameter X. The decision rule δ can be then expressed as a function of Γ given by (Poor, 1988)

$$\delta(y) = \begin{cases} 1 \text{ if } x \in \Gamma_1 \\ 0 \text{ if } x \in \Gamma_0 \end{cases} \tag{5.2}$$

so that the value of δ for a given $x \in \Gamma$ is the index of the hypothesis accepted by δ.

In order to choose Γ_1 in some optimum way, different statistical methods are available such as Bayesian and Neyman-Pearson hypothesis testings (Poor, 1988). In the Bayesian formulation, the optimality in testing is defined in terms of minimizing the overall expected cost which can be interpreted as the average risk. However, in many problems of practical interest, defining a specific cost structure on the decision made in testing is not possible and/or desirable. An alternative design criterion, which can address such cases, is available and is known as the Neyman-Pearson criterion (Poor, 1988). This design criterion was previously applied in radar systems where the concepts of false alarm and detection rate were defined as the system performance metrics. For the safety application problem defined in this chapter, the Neyman-Pearson formulation is the appropriate criterion and has been used for the first time.

5.4.1 **Neyman-Pearson Hypothesis Testing**

In testing H_0 versus H_1 there are two types of errors possible: H_0 can be falsely rejected or H_1 can be falsely rejected. The former error is called a *Type I* error or a false alarm and the latter is called a *Type II* error or a miss. Correct acceptance of H_1 is similarly called detection. For a decision rule δ, the probability of a *Type I* error is known as the false-alarm probability (or false-alarm rate) of δ, and is denoted by $P_F(\delta)$. Similarly the probability of a *Type II* error is called the miss probability, $P_M(\delta)$. However, in discussing the latter quantity the detection probability $P_D(\delta) = 1 - P_M(\delta)$ is usually considered (Poor, 1988).

Note that the design of a test for H_0 versus H_1 involves a trade-off between the probabilities of the two types of errors, since one can always be made arbitrarily small at the expense of the other. For making this trade-off, the Neyman-Pearson criterion considers the minimization of the miss probability subject to a constraint on the false-alarm probability. The Neyman-Pearson design criterion is therefore given by:

$$\max_{\delta} P_D(\delta) \text{ subject to } P_F(\delta) \le \alpha \tag{5.3}$$

where α is a defined bound on the false-alarm probability and is known as the significance level of the test. Note that, unlike Bayesian criterion, the Neyman-Pearson criterion recognizes a basic asymmetry in importance of the two hypotheses. This is particularly crucial in the proposed safety application problem where the reliability of the system is more characterized by the detection probability rather than the false alarm probability.

It can be shown that for a binary hypothesis problem with continuous probability distributions, and assuming that $\alpha, \eta > 0$, the Neyman-Pearson decision rule can be obtained as (Poor, 1988):

$$\delta(x) = \begin{cases} 1 & \text{if } \dfrac{p_1(x)}{p_0(x)} \geq \eta \\ 0 & \text{if } \dfrac{p_1(x)}{p_0(x)} < \eta \end{cases} \tag{5.4}$$

where p_0 and p_1 are respectively the conditional probability density functions (pdf) correspond to the two hypotheses probability distributions P_0 and P_1. The optimum threshold η in Equation (5.4) can be then calculated by solving (Poor, 1998)

$$P_F(\delta) = \alpha \tag{5.5}$$

5.4.2 **The Optimum Algorithm for the Proposed Safety System**

In the proposed safety system, H_0 is the hypothesis that the true location coordinate of the tag (i.e., x_t) is within the vicinity zone and H_1 is the hypothesis that x_t is within the caution zone. Therefore, the conditional pdfs of the observed location coordinate (i.e., x) given the corresponding hypotheses can be written as

$$p_0(x) = p(x \mid H_0) \tag{5.6}$$

$$p_1(x) = p(x \mid H_1) \tag{5.7}$$

Recall the relationship between the observed and the true locations, i.e.,

$$x = x_t + E_x(x_t, y_t) \tag{5.8}$$

where $E_x(x_t, y_t)$ the observation error which is a function of the true location coordinates (x_t, y_t). The results of the error modeling phase have demonstrated that the statistical behaviour of this error at the center of each grid follows a Normal distribution given by:

$$E_x(x_t, y_t) \sim N(\mu(x_t, y_t), \sigma(x_t, y_t)) \tag{5.9}$$

Assuming that the distribution of the error for any true location (x_t, y_t) within a grid can be approximated by the distribution of the error at the center of that grid (x_t^c, y_t^c), the conditional pdf of the observed location coordinate x given the true location (x_t, y_t) can be obtained using Equations (5.8) and (5.9) as the Normal distribution $N(x_t + \mu(x_t^c, y_t^c), \sigma(x_t^c, y_t^c))$ and is given by

$$p(x \mid x_t, y_t) = \frac{1}{\sqrt{2\pi\sigma^2(x_t^c, y_t^c)}} e^{-\frac{(x - x_t + \mu_E(x_t^c, y_t^c))^2}{2\sigma^2(x_t^c, y_t^c)}} \tag{5.10}$$

To design an optimum algorithm for the proposed safety system based on the Neyman-Pearson criterion, the parameter α, which is the maximum false alarm rate that can be tolerated, should be known. Then, subject to the constraint imposed by α, the detection rate is maximized (i.e., the miss rate is minimized) by solving the Neyman-Pearson optimization problem in Equation (5.3). Note that the solution of this optimization problem which is given by Equation (5.4) can be equivalently expressed as:

$$\delta(x) = \begin{cases} 1 & \text{if} \quad x \le x_{th} \\ 0 & \text{if} \quad x > x_{th} \end{cases} \tag{5.11}$$

where x_{th} is the corresponding threshold parameter. Comparing to Equation (5.4), the direction of the inequalities in Equation (5.11) is reversed since $p_1(x)/p_0(x)$ is a decreasing function of x according to the geometry of the proposed safety system as depicted in Figure 34. Using Equation (5.5), the threshold parameter x_{th} can be obtained by solving

$$P_F(\delta) = P_0(x \le x_{th}) = \int_0^{x_{th}} p_0(x)dx = \alpha \tag{5.12}$$

where $p_0(x)$ can be obtained by inserting Equation (5.10) into Equation (5.6). Furthermore, having x_{th} from Equation (5.12), the detection probability can be obtained as

$$P_D(\delta) = P_1(x \le x_{th}) = \int_0^{x_{th}} p_1(x)dx \tag{5.13}$$

where $p_1(x)$ can be obtained by inserting Equation (5.10) in Equation (5.7).

Figure 43 shows different steps to find the optimum threshold value (x_{th}) where x_{th}^0 is the initial threshold value which can be assumed as the coordinate of the hazardous border.

Note that the Neyman-Pearson decision rule given by Equation (5.11) designs a very simple alarming algorithm which is optimum according to the Neyman-Pearson criterion. Based on this optimum algorithm, the system decides whether or not to alarm by comparing the real-time observed location coordinate x with the optimum threshold parameter x_{th}. The flowchart of this algorithm is shown in Figure 44.

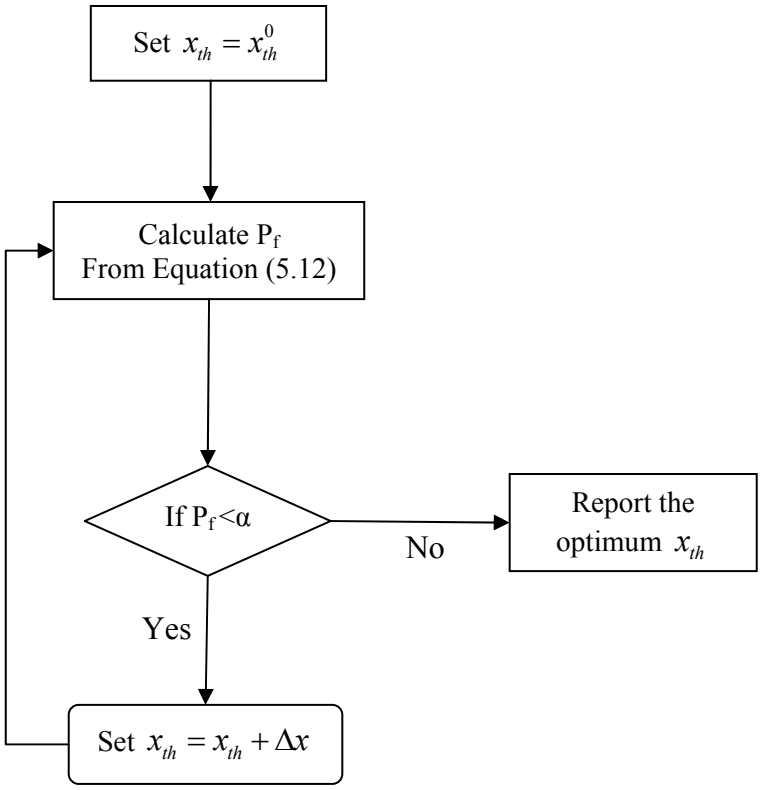

Figure 43: Different steps to find the optimum threshold parameter (x_{th}).

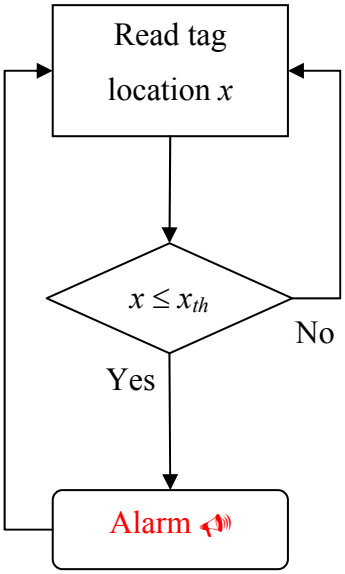

Figure 44: The flowchart of the optimum warning system.

5.5 Numerical Performance Evaluation

Based on the statistical analysis presented in the last section, the performance of the proposed safety system can be numerically evaluated. In these numerical results, it is assumed that the caution zone is defined from $x = 3$ m to $x = 4$ m and the vicinity zone is defined from $x = 4$ m to $x = 5$ m. Figures 45 and 46 show the variation of the detection rate and the optimum threshold parameter x_{th} obtained through Neyman-Pearson criterion versus the design parameter α. Using these two figures, one can obtain the optimum threshold parameter required for the alarming process and the optimum performance of the system in terms of the detection rate for any predefined value of α. It can be observed that setting higher bounds on the false alarm rate (i.e., α), the detection rate increases and the optimum threshold parameter moves away from the caution zone.

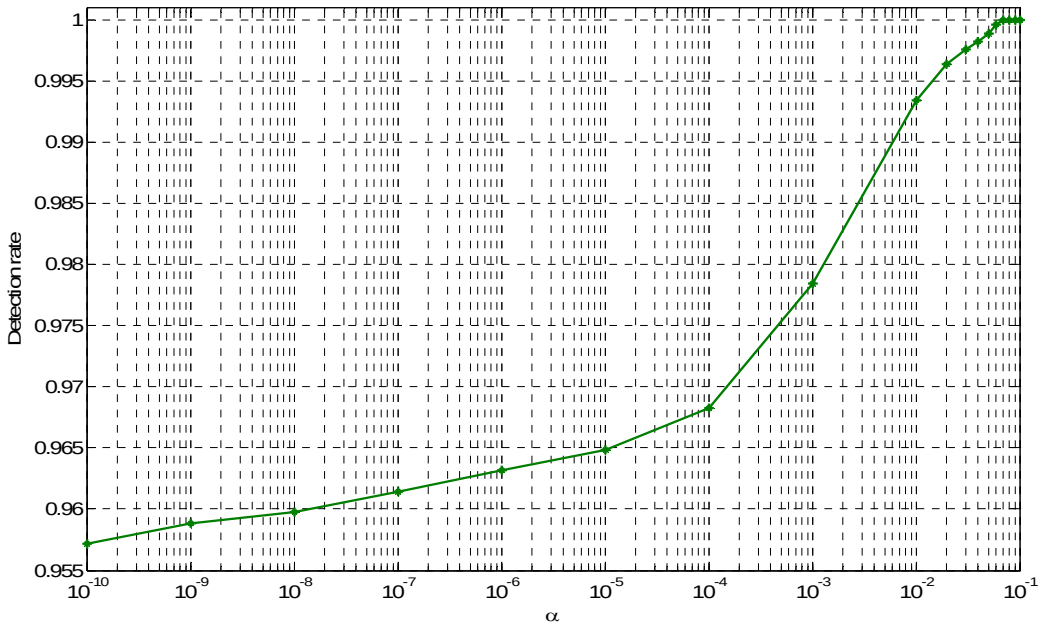

Figure 45: Variation of the detection rate versus the design parameter α.

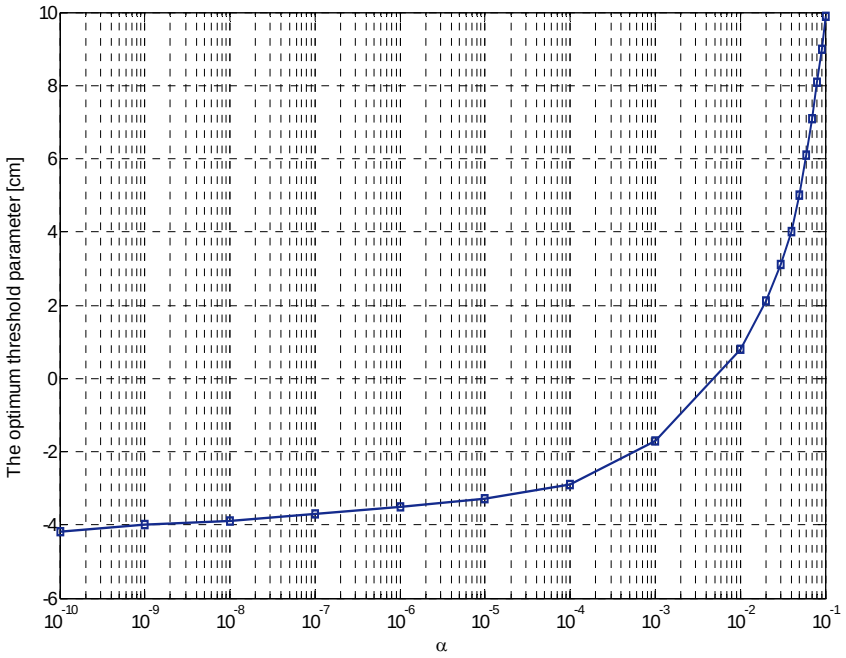

Figure 46: Variation of the optimum threshold parameter versus the design parameter *α*.

Note that in the numerical results, the value of the optimum threshold parameter is represented as the deviation from the border line of the caution and vicinity zones at $x = 4$ m (i.e., $x_{th} - 4$) rather than its original value.

Figure 47 illustrates the trade-off between miss rate and false alarm rate versus the variation of the threshold parameter. Therefore, decreasing the miss rate involves increasing the false alarm rate and vice versa. It is further observed that an increase in the deviation of x_{th} from the border of the caution zone and the vicinity zone results in a higher false alarm rate and equivalently a lower miss rate.

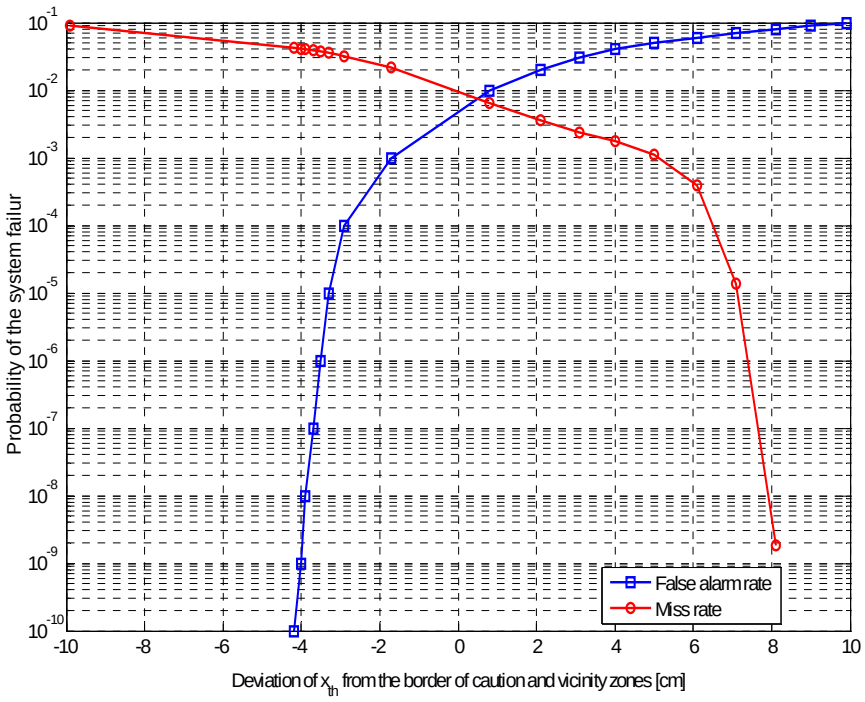

Figure 47: The miss and false alarm probability versus optimum threshold parameter x_{th}.

5.6 Summary

In this chapter, the application of UWB technology in an automated safety system has been investigated. In the first phase, an error modeling of a UWB system in a lab environment was conducted. The area under coverage was divided into grids and the location of a tag at the center of each grid was recorded. The calculated error samples were employed to model the statistical behaviour of the system in the underlying environment. The variation of the average and standard deviation of the error coordinates over the covered area was studied. In the second phase, a statistical analysis has been performed to design an optimum automated safety system. The reliability of this system was defined based on some performance metrics such as

miss rate, detection rate, and false alarm rate. Based on the Neyman-Pearson hypothesis testing, an alarm algorithm has been proposed using an optimum threshold-based decision rule. Numerical evaluation of the performance of the proposed system shows that setting higher bounds on the false alarm rate, the optimum detection rate increases. It is also shown that there is a trade-off between miss rate and false alarm rate as the optimum threshold parameter varies, therefore, decreasing the miss rate involves increasing the false alarm rate and vice versa.

Chapter 6

Conclusions

Application of a UWB sensing technology for position location in indoor construction environments has been studied in this research. This research was inspired by studies, which demonstrated that tracking and locating technologies are very beneficial to a project manager in order to conduct different construction phases on time, safer, and within the allocated budget. UWB sensing technology is considered as a real-time data acquisition technique. The need for evaluating the application of such a system in construction projects led to assess the performance of the system in a real construction environment. The accuracy of a UWB system in a laboratory environment and also in a construction site was investigated. The experimental results and the real project challenges were used to make recommendations for using a UWB positioning system. This study has successfully addressed the challenges that might be expected for installing a UWB sensing system in a construction site and provided experience to compensate for the potential delays and problems associated with its use. The use of a UWB system in safety application was investigated and the steps for designing a warning system have been proposed.

6.1 Contributions

This research has three major contributions:

1) A contribution in the overall performance evaluation of the UWB sensing technology in civil engineering construction industry.
2) A contribution in the use of UWB position location system in a real construction project.
3) A contribution in the use of UWB positioning system in safety applications.

The significant findings associated with these contributions are as follows:

1. This study provided an evaluation of a UWB system performance in indoor environments. The effect of different construction materials on the system accuracy was investigated. It was found that metallic surfaces highly interfere with the system and decrease the system accuracy because of the multipath effect associated with them.
2. The effect of different material covers (no cover, wood, metal, and RF-shield box) on the systems accuracy was investigated and the results were as below:
   - Average error (E_{xyz}) for the tag readings, comparing to their true location measured by total station equipment was 13.1 *cm* without cover and 12.2 *cm* for the wood cover, which were pretty close to each other. On the other hand, the systems accuracy for the other two covers (i.e., metal and RF-shield boxes) was lower. The calculated average error (E_{xyz}) for the metal box was 44.9 *cm* and for RF-shield box was 45.1 *cm*. These two values show that the systems behaviour for the tags under metal box cover is similar to that for the RF-shield box.

- The scatter plot of E_y vs. E_x for wood box and RF-shield box illustrated that, in the case of metal box the data was more scattered; that was interpreted as the effect of multipath caused by the metal surface.

3. This study showed that a UWB measurement accuracy is highly depends on the line of sight of the point to be located and the position of the UWB receivers covering the area.
   - The receivers should not be blocked by metallic surfaces since they affect the systems accuracy by producing multipath effect.
   - Rectangular deployment is the best recommended layout.
4. Different challenges associated with installing a UWB system in a construction environment and some recommendations have been addressed. Some of the important issues were:
   - Systems power supply
     - Better to be separated from the power supply used for the construction which may be prone to shut down. This will avoid repeated calibration and the readings will be more consistent.
   - Receiver connections
     - Better to be wireless since it is hard to run long cables in a changing environment construction site.
   - Cabling issues
     - Better to use manufactured and tested cables to reduce and diagnose connection-related problems.
     - Better to use network and timing combiner accessory to reduce the length and the cost of running cables.

- Data acquisition software
  - Better to use an external router to assign IP addresses to the receivers instead of using a DHCP server program which is incompatible with some operating systems like Windows Vista®.
- Layout of the receivers
  - Better to be rectangular since the system can use the AOA and TDOA principles more effectively.
  - Better to consider the future changes in construction site environment to avoid any system shut down and to maintain the system for a longer period.

5. The lowest average error in the lab environment (Chapter 3) was 12-13 *cm* (E_{xyz}), and in the construction site (Chapter 4) was 48 *cm* (E_{xy}) for floor points, 35 *cm* (E_{xy}), and 53 *cm* (E_{xyz}) for pipe points.
6. Error modeling in a UWB system covered area in order to compensate the systematic error was conducted and recommendations about the grid layout to better understand the systems behaviour have been made.
7. The application of UWB technology in an automated safety system has been investigated and a design for a UWB warning system has been proposed based on Neyman-Pearson hypothesis testing criterion.
8. Numerical evaluation of the performance of the proposed system showed that setting higher bounds on the false alarm rate, the optimum detection rate increases. It is also shown that there is a trade-off between miss rate and false alarm rate as the optimum threshold parameter varies, therefore, decreasing the miss rate involves increasing the false alarm rate and vice versa.

6.2 Recommendations for Future Research

Some directions for future works can be recommended as:

1. It is suggested to repeat Chapter 3 study in a bigger scale to investigate the effect of different construction materials. It is better if the covering material only blocks the top surface of the tag. Leaving the other sides of the tag open, makes the model more realistic. Although it rarely happens in a construction site that a tag be isolated by a special material, but it is common that a material in the vicinity of the tag affects the systems readings. The effect of a concrete cover is good to be investigated.
2. The data collected from the construction site has been employed in Chapter 4 to study the accuracy of UWB system in a construction site. This data can be also investigated to demonstrate the efficiency of an automated UWB system for the progress tracking of pipe installation. It can be further combined with the other sources of information such as laser scanner, photogrammetry, and RFID to give a general perspective of the construction progress. As proposed in (Shahi, 2010), the combined information using a fuzzy logic inference system results in a more accurate automated system for progress tracking of the construction site.
3. As mentioned in Chapter 5, an adaptive grid layout (with available grid spacing) of the UWB system covered area can be considered as a useful method to optimize the error modeling of a UWB system. This can be investigated as a future work. In this process, the average error of the UWB system is recorded for a regular grid layout in the first phase; then for the grid

regions where the variation of the average error is higher, the process is repeated with denser grids. This makes a better understanding of the system behaviour in the whole covered area.

4. In Chapter 5, a rectangular geometry is considered for the hazardous zone. However, different geometries of the hazardous zone can be considered as future research. For some of these cases, it might be required to obtain an optimum threshold curve rather than the optimum threshold parameter. The effects of the tag carriers' moving speed and the UWB system update rate on the performance of the proposed automated safety system can be also studied in the future.
5. An alarm system hardware can be developed based on the proposed design for the UWB warning system in this study.

References

Bennet &Rosst, C. L., and G. F., Ross., (1978). "Time-Domain Electromagnetics and its Applications". Proceedings of the IEEE, Vol. 66, pp. 299–318.

Bowes & Keefer, A., and C. Keefer., (2007). "Joint Rapid Airfield Construction". Trimble Dimensions 2007 Annual Conference, Las Vegas, Nev., 5–7.

Breed, G., (2005). "A Summary of FCC Rules for Ultra Wideband Communications". High Frequency Electronics, pp. 42–44.

Ghavami et al., M., Michael, L. B., and Kohno, R., (2007). "Ultra Wideband Signals and Systems in Communication Engineering". 2nd ed., Chichester, West Sussex, England: John Wiley & Sons.

Golparvar Fard, M., and Peña-Mora. F., (2007). "Semi-Automated Visualization of Construction Progress Monitoring". Proc., Construction Research Congress 2007, Freeport, Bahamas.

Gu X., and Taylor L., (2003). "Ultra-wideband and its Capabilities'. BT Technology Journal, Vol 21, pp: 56-66.

Montgomery, D. C., (2001). "Design and Analysis of Experiments". 5th ed USA: John Wiley & Sons.

Munoz, D., Bouchereau, F., Vargas, C., Enriquez-Caldera, R., (2009). "Position Location Techniques and Applications". USA: Elsevier.

Poor H. V., (1988). "An Introduction to Signal Detection and Estimation". New York: Springer- Verlag.

Razavi et al., S. N., Haas, C. T., Vanheeghe, P., and Duflos, E., (2009). "Real World Implementation of Belief Function Theory to Detect Dislocation of Materials in Construction". 12th International Conference on Information Fusion, Seattle, WA, USA, pp: 748-755.

Shahi A., (2010). “Activity-Based Data Fusion for Automated Progress Tracking of Construction Projects”, PhD Proposal, University of Waterloo, Canada.

Siwiak, K., McKeown, D., (2004). “Ultra-wideband Radio Technology”. Chichester, West Sussex, England: John Wiley & Sons.

Song, J., C. Haas, and C. H. Caldas., (2006). “Tracking the Location of Materials on Construction Job Sites”. Journal of Construction Engineering and Management, Vol. 132, No. 9, pp: 911–918.

Teizer J., Venugopal M., and Walia A., (2008). “Ultrawideband for Automated Real-time Three-Dimensional Location Sensing for Workforce, Equipment, and Material Positioning and Tracking”. Transportation Research Record, Transportation Research Board of the National Academies, Washington D.C, 2081: 56-64.

Teizer J., Lao D., and Sofer M., (2007). “Rapid Automated Monitoring of Construction Site Activities Using Ultra-Wideband”. 24th international Symposium on Automation & Robotics in Construction (ISARC), Madras, Oregon, USA, Proc. 24th ISARC: 23-28.

Teizer, J., Caldas C.H., and Haas, C.T. (2007). “Real-Time Three-Dimensional Occupancy Grid Modeling for the Detection and Tracking of Construction Resources”. Construction Engineering and Management, 133(11), pp. 880-888.

Teizer, J., Kim, C., Haas, C.T., Liapi, K.A., and Caldas, C.H. (2005). “A Framework for Real-time 3D Modeling of Infrastructure”. Transportation Research Record, No. 1913, pp. 177-186.

Ubisense® Company, (2011), Product Fact Sheets, http://www.ubisense.net/en/, accessed on 28 May 2011.